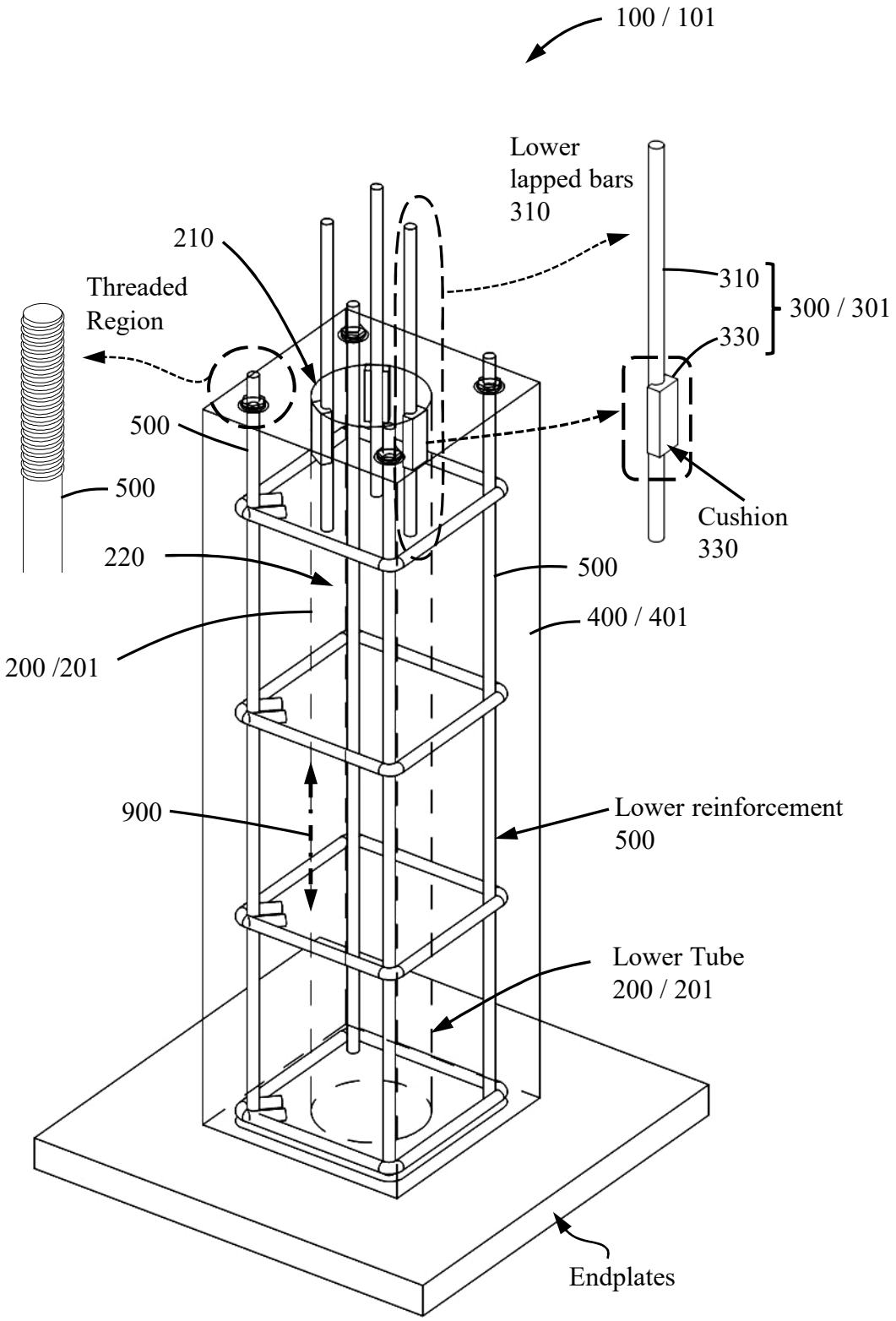

Lower column

Fig. 1A

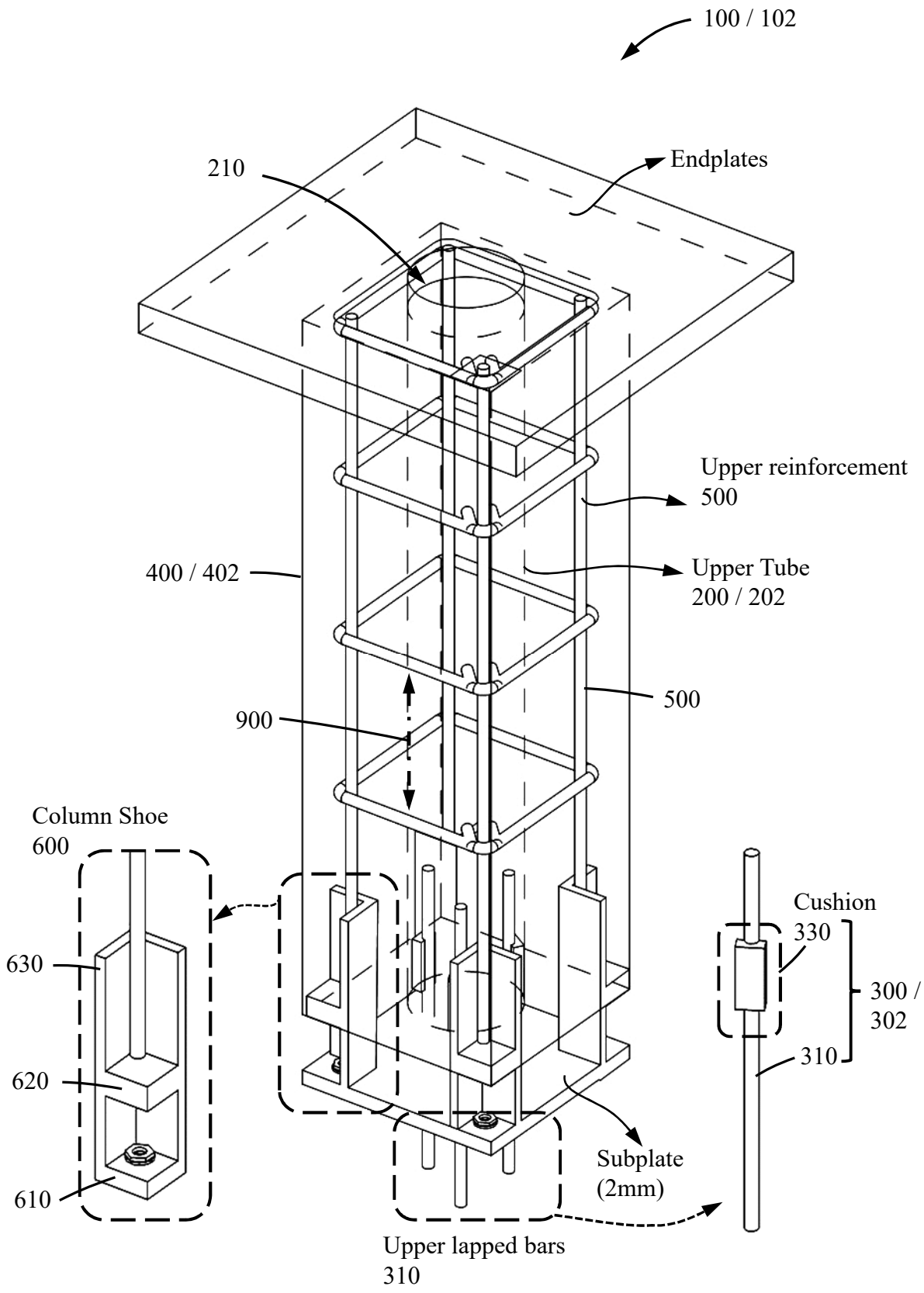
100 / 102
210
Endplates
Upper reinforcement
500
400 / 402
Upper Tube
200 / 202
500
900
Column Shoe
600
630
620
610
Cushion
330
300 /
302
310
Subplate
(2mm)
Upper lapped bars
310

Fig. 1B

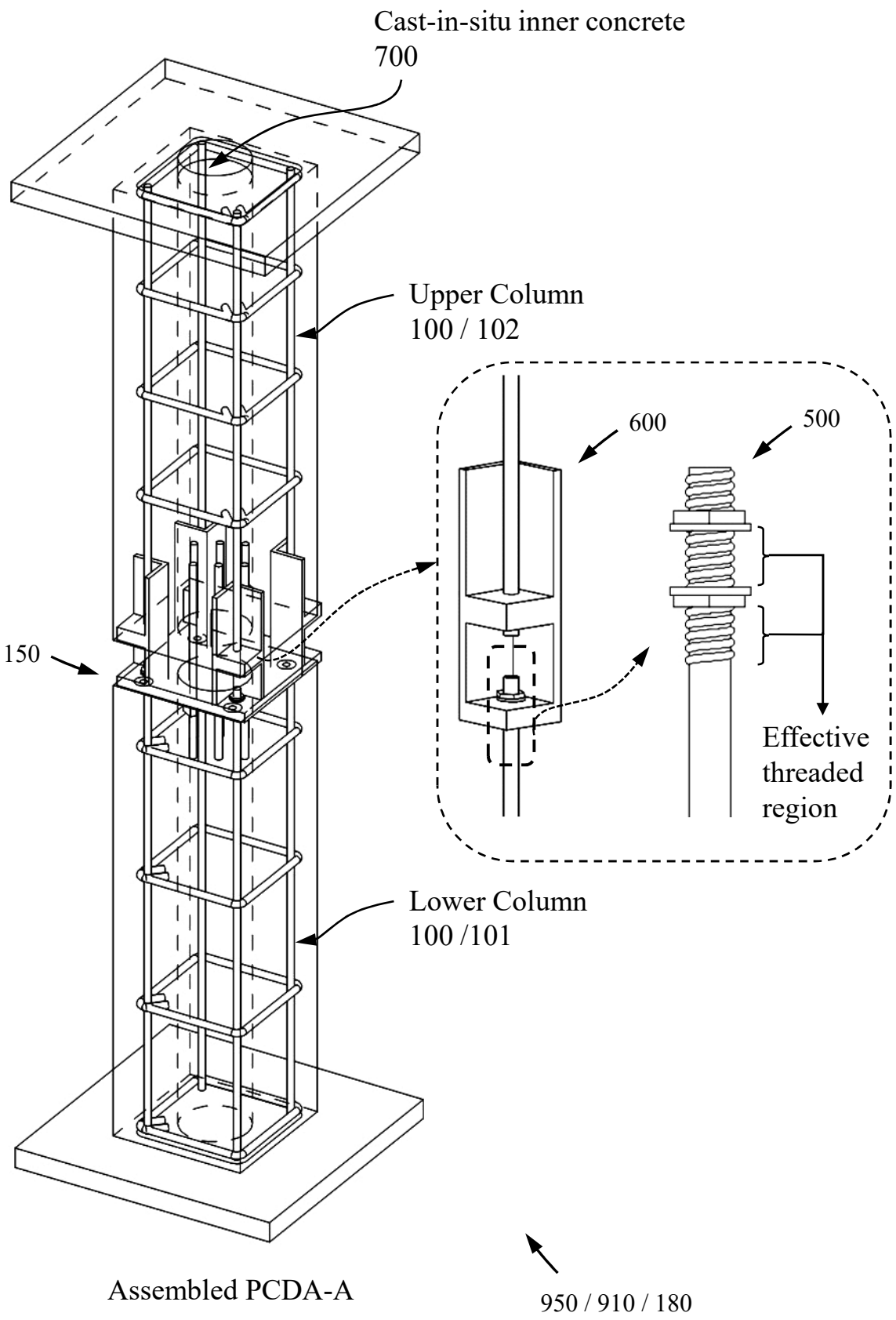
Cast-in-situ inner concrete
700
Upper Column
100 / 102
600
500
150
Effective
threaded
region
Lower Column
100 /101
Assembled PCDA-A
950 / 910 / 180

Fig. 1C

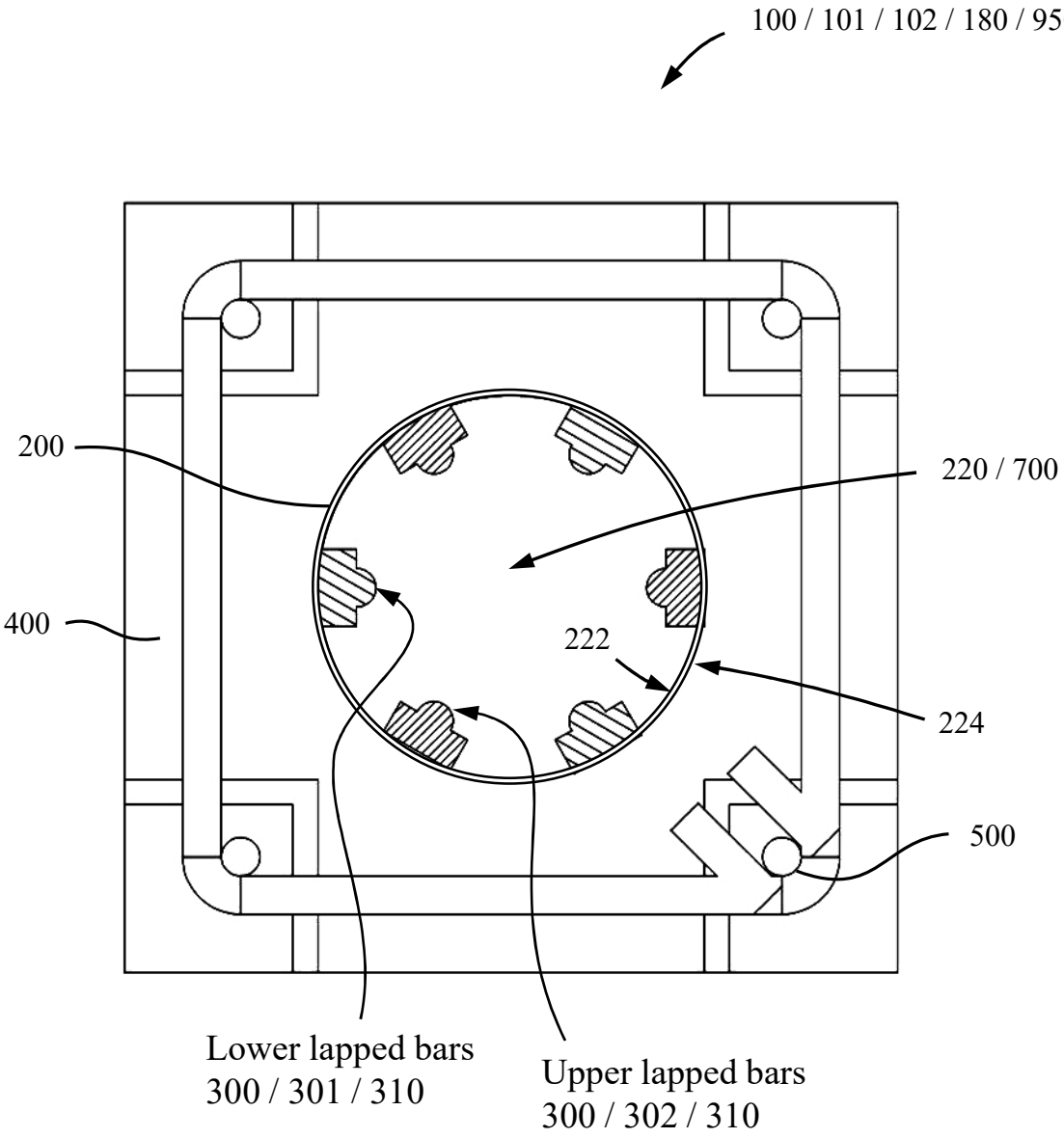

Cross-sectional view of assembled PCDC-A

Fig. 1D

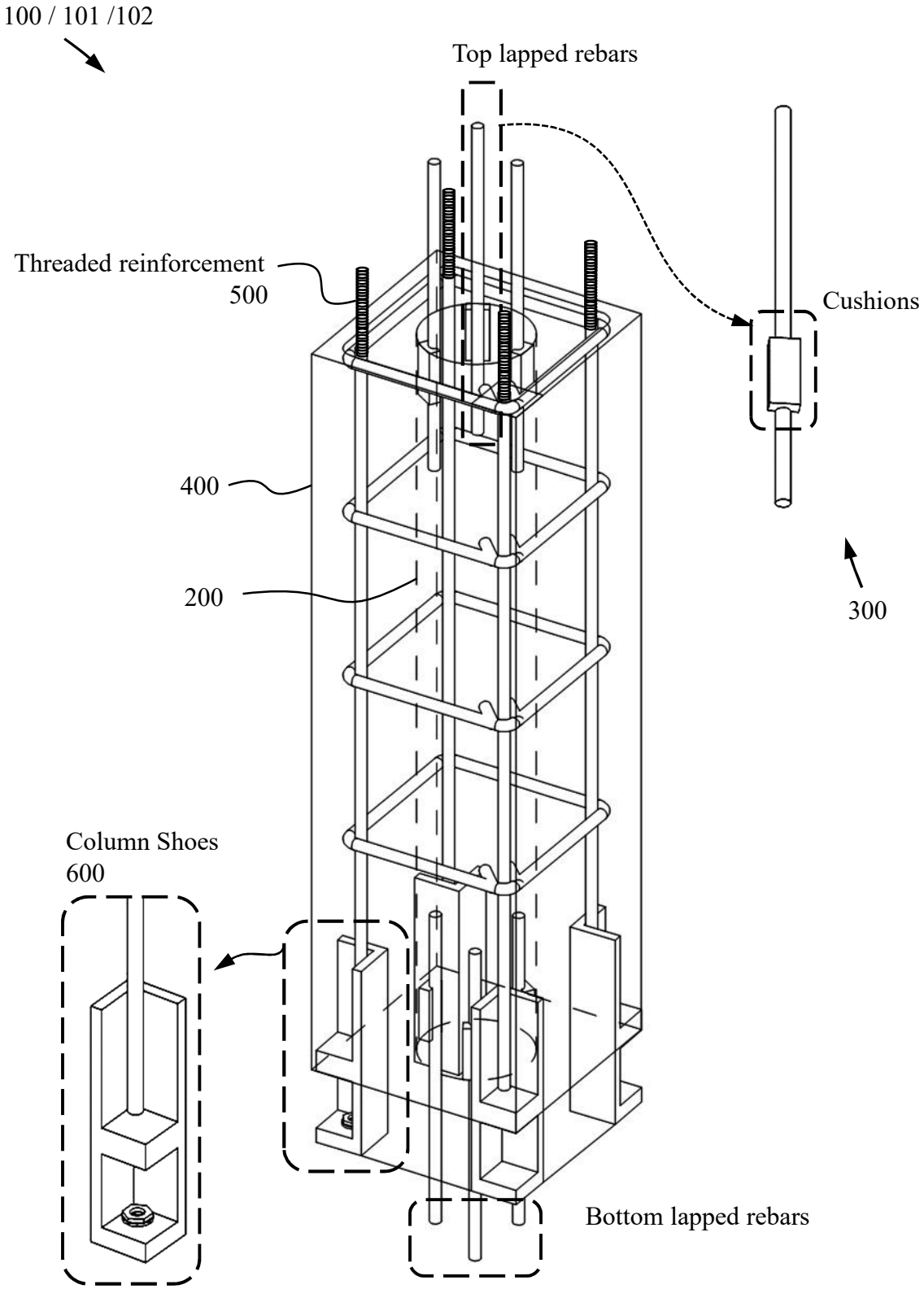

Overview of precast column segment (PCS)

Fig. 1E

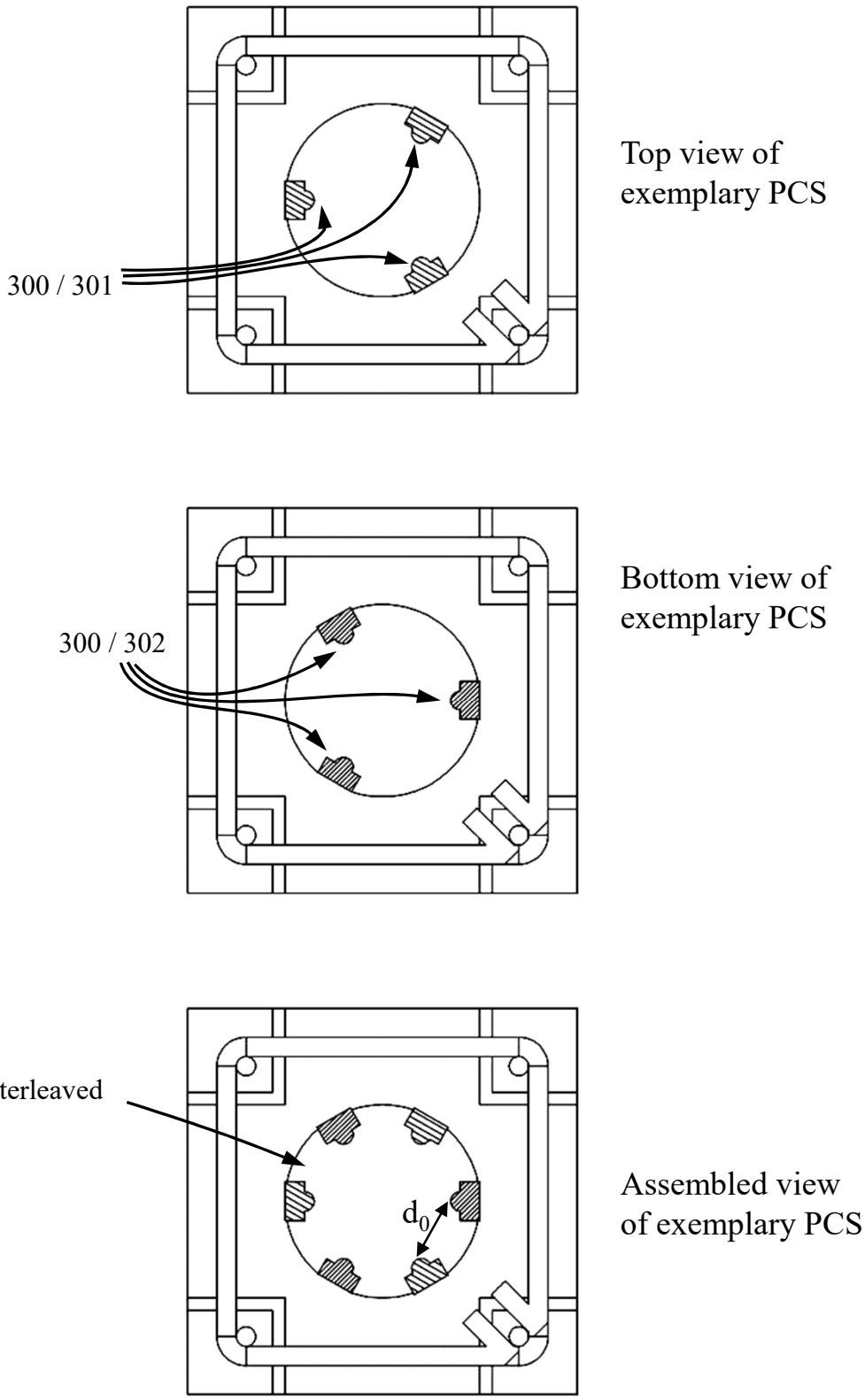
300 / 301
Top view of exemplary PCS
300 / 302
Bottom view of exemplary PCS
Interleaved
d_0
Assembled view of exemplary PCS

Fig. 1F

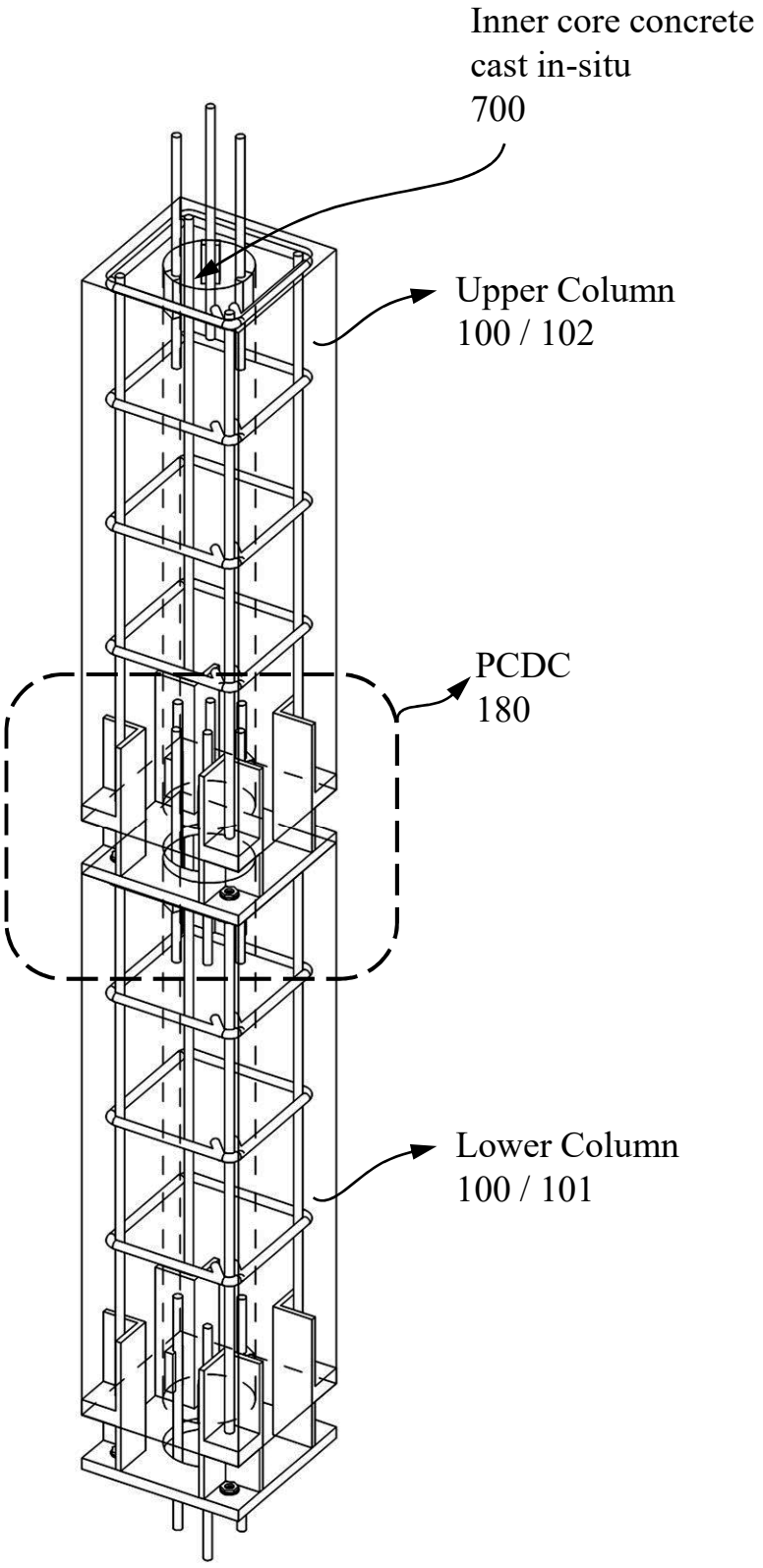
Inner core concrete
cast in-situ
700
Upper Column
100 / 102
PCDC
180
Lower Column
100 / 101

Fig. 1G

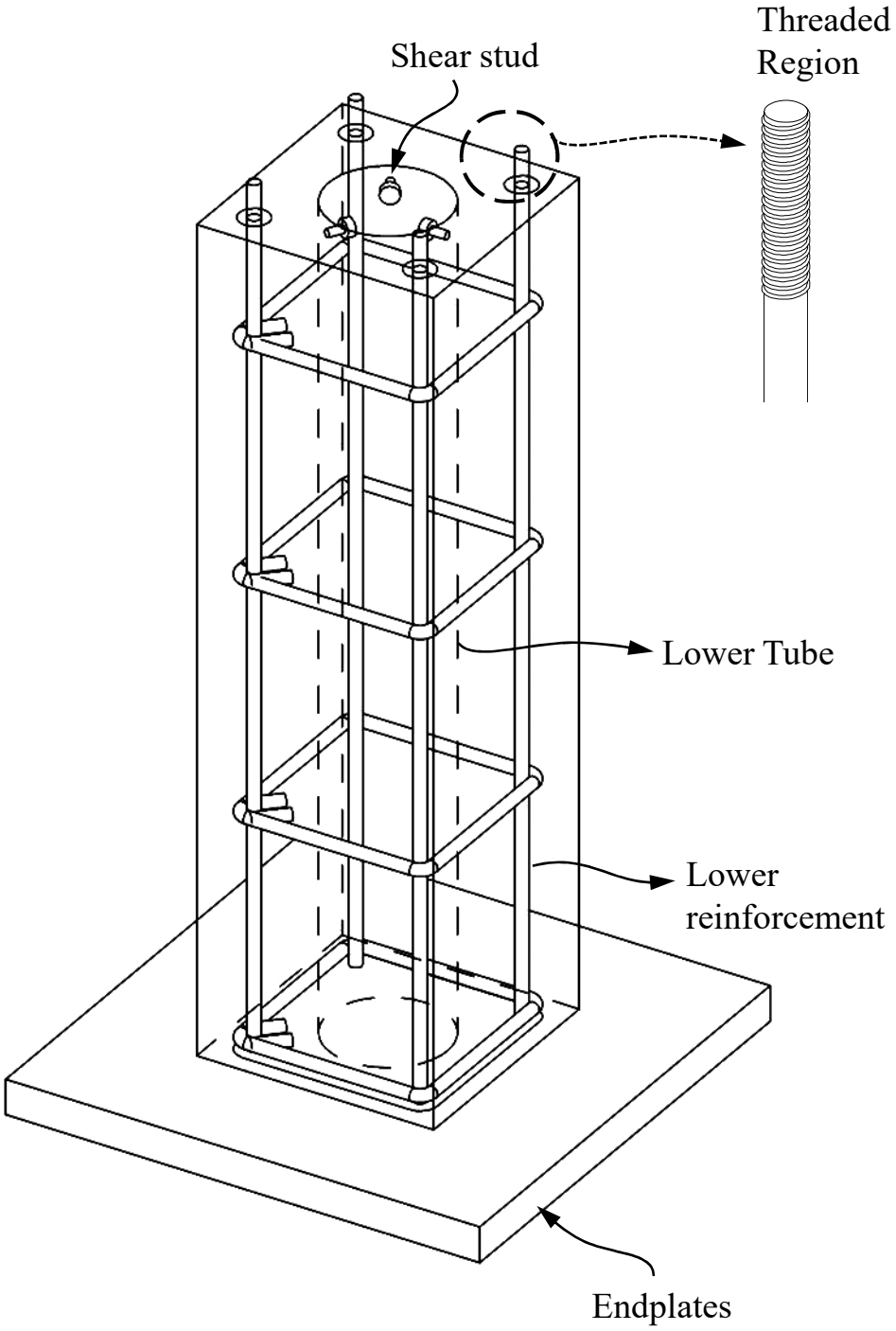
Threaded
Region
Shear stud
Lower Tube
Lower
reinforcement
Endplates

Fig. 2A

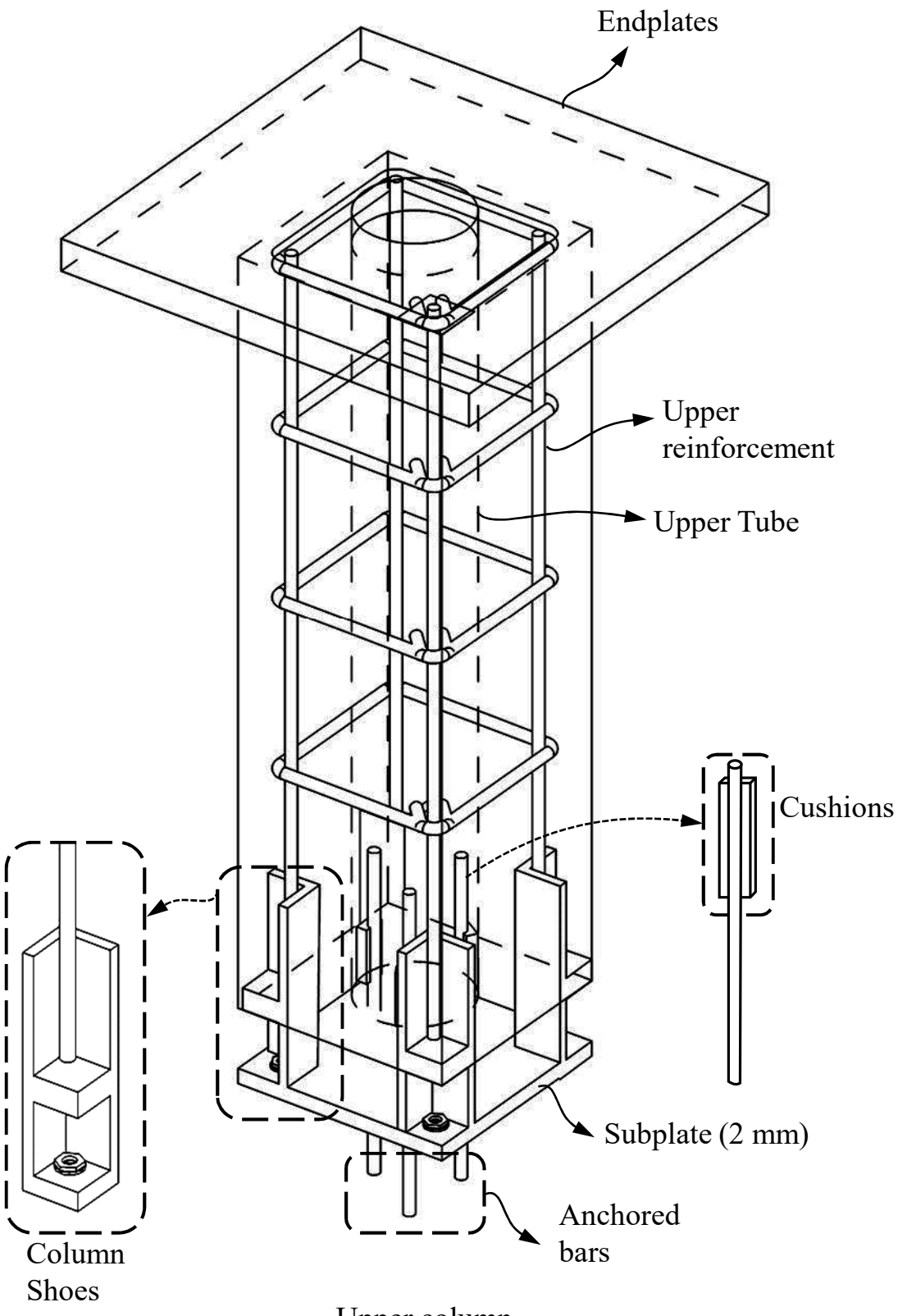
Endplates
Upper
reinforcement
Upper Tube
Cushions
Subplate (2 mm)
Anchored
bars
Column
Shoes
Upper column

Fig. 2B

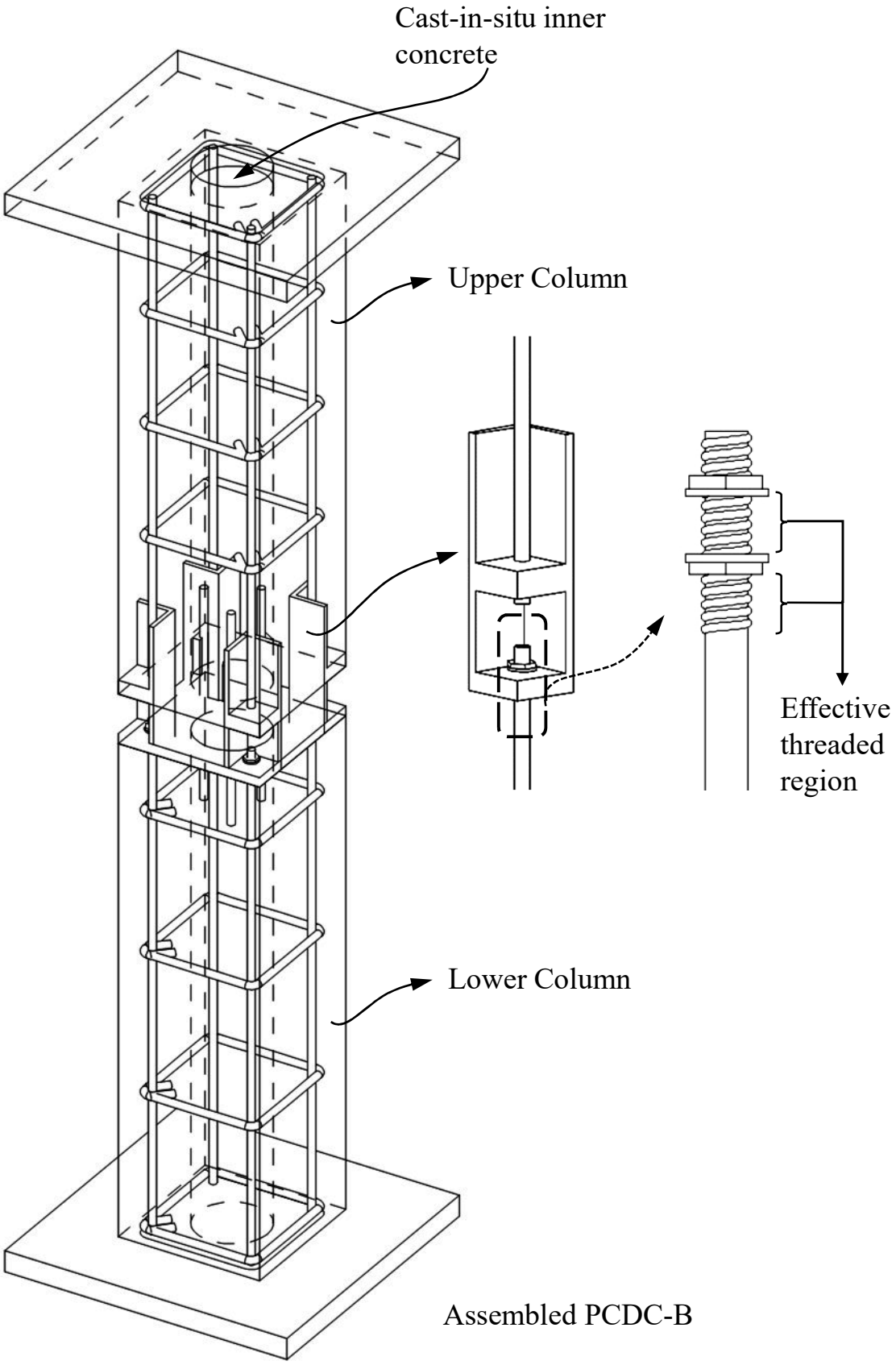

Assembled PCDC-B

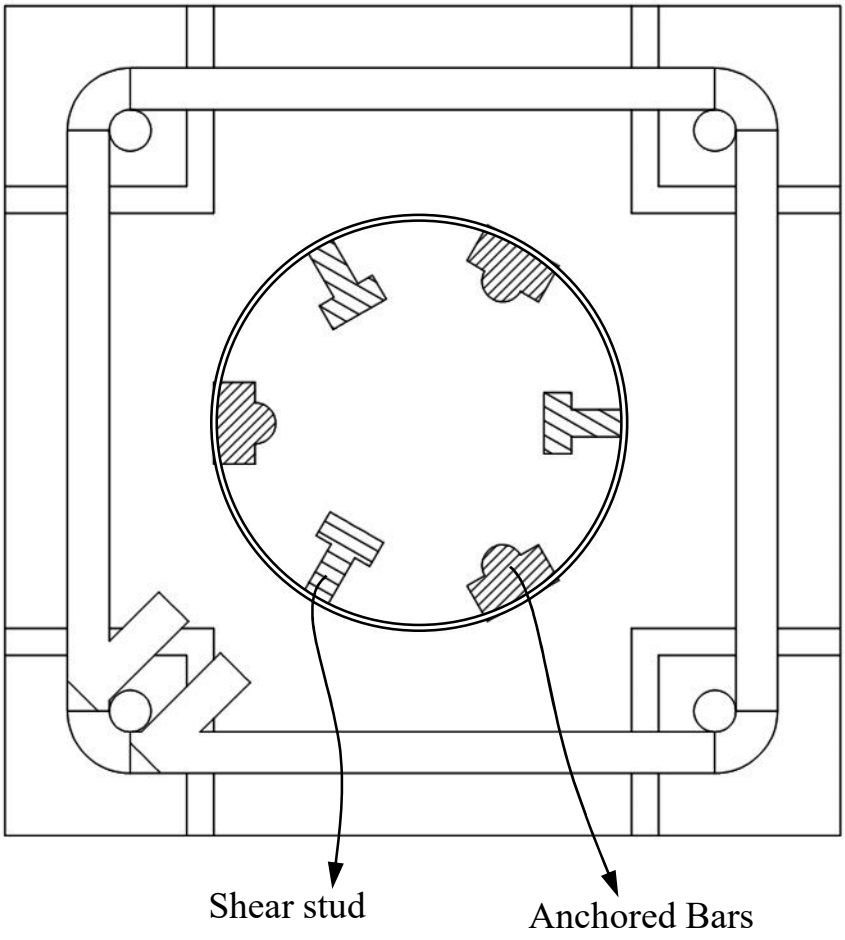

Cross-sectional view of assembled PCDC-B

Fig. 2D

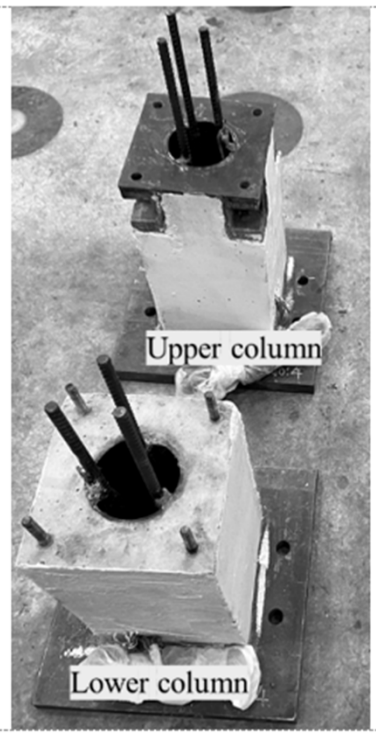

(a) PCDC-A

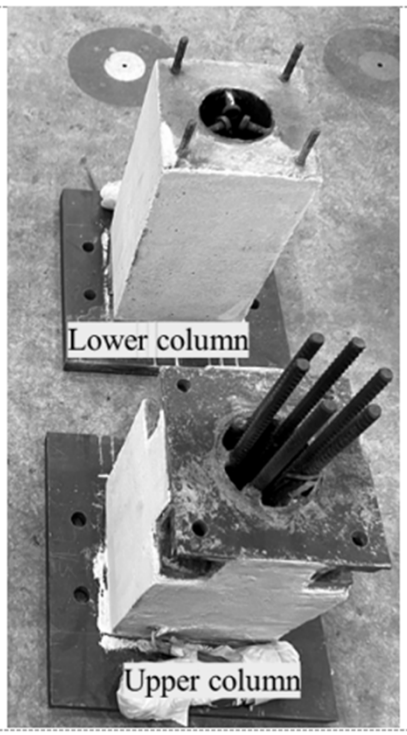

(b) PCDC-B

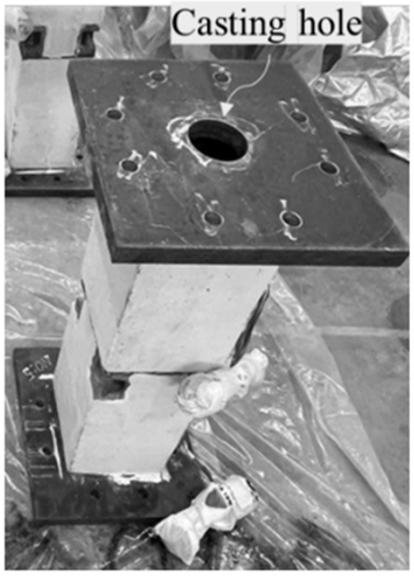

(c) Connection assembly

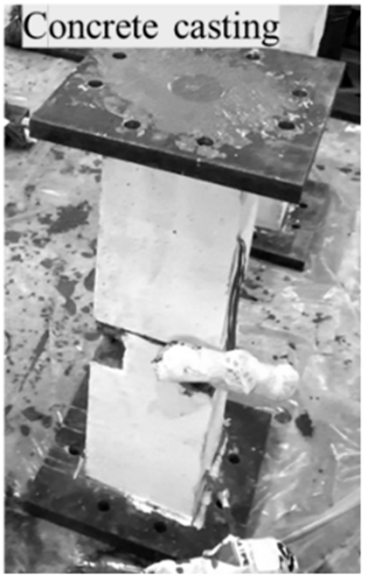

(d) On-site concrete casting

Fig. 3

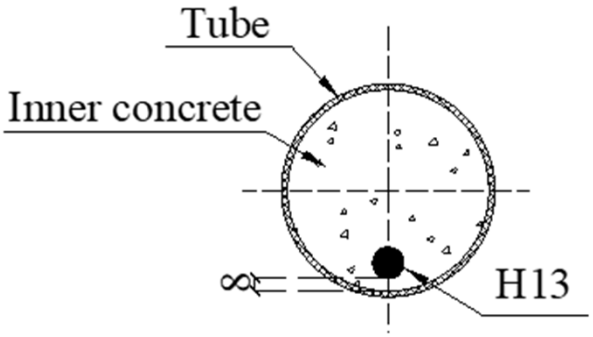

(a) Concentric pullout specimens-CP

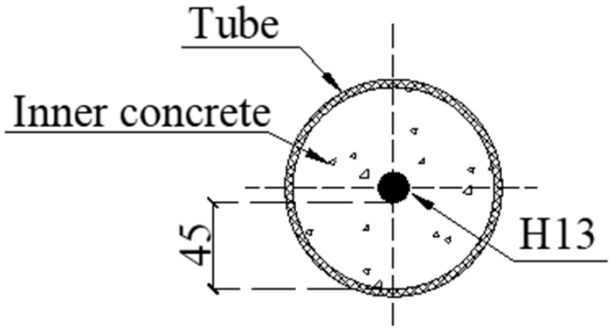

(b) Eccentric pullout specimens-EP

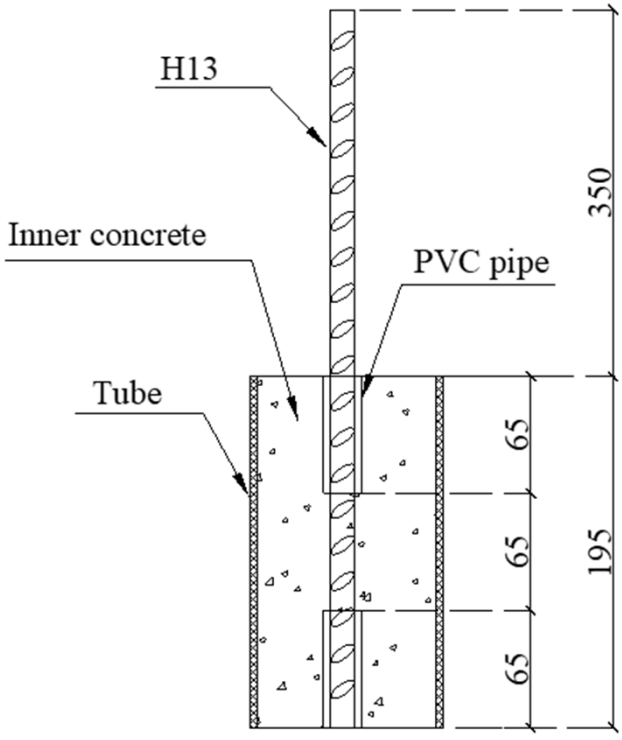

(c) Elevation view of pullout specimens

Fig. 4

Dimensions of test specimens: (a) CFST-R; (b) CFST-A; (c) CFST-B

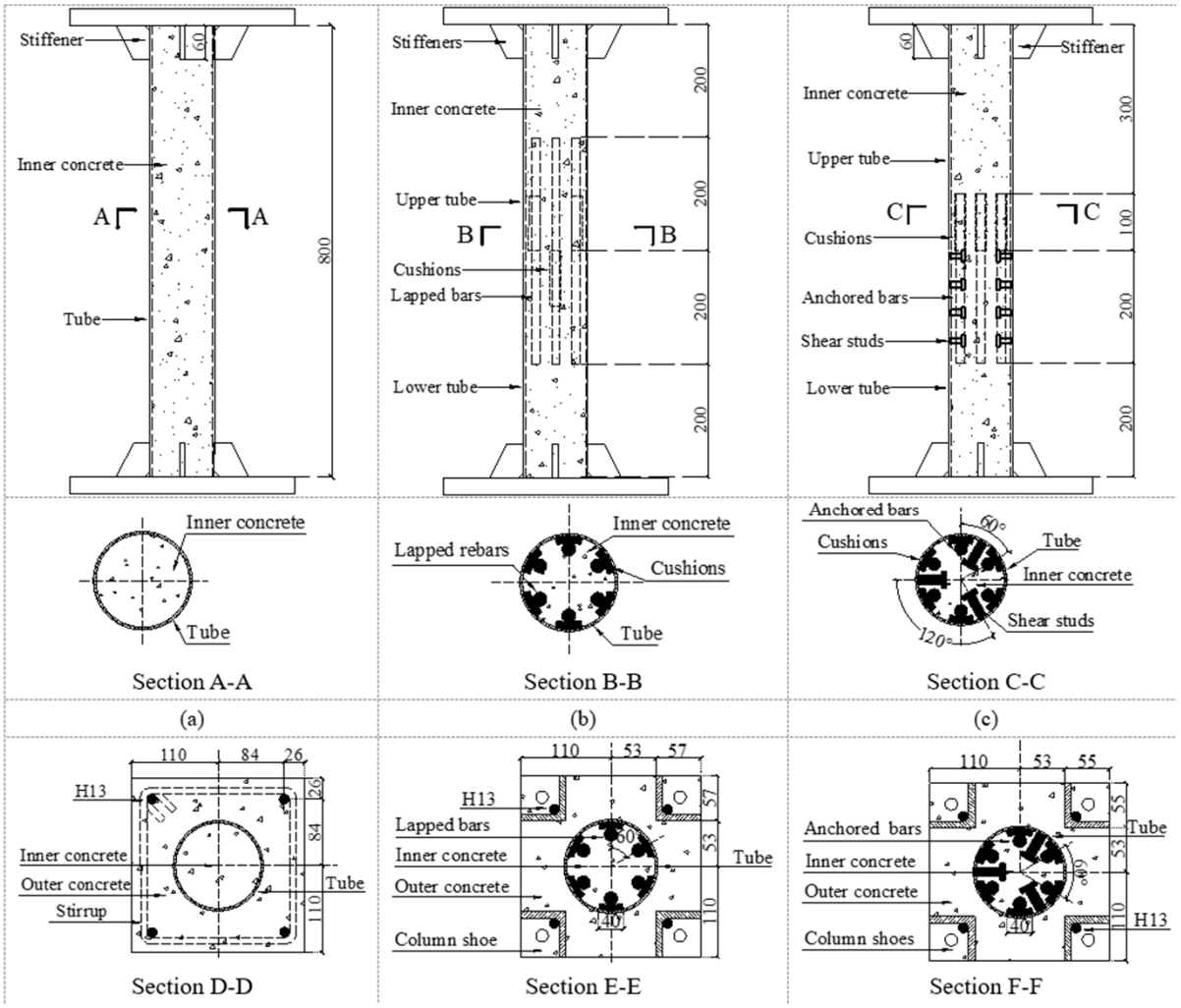

Fig. 5A **Fig. 5B** **Fig. 5C**

Fig. 5 Dimensions of test specimens: (d) CECFST-R; (e) CECFST-A; (f) CECFST-B

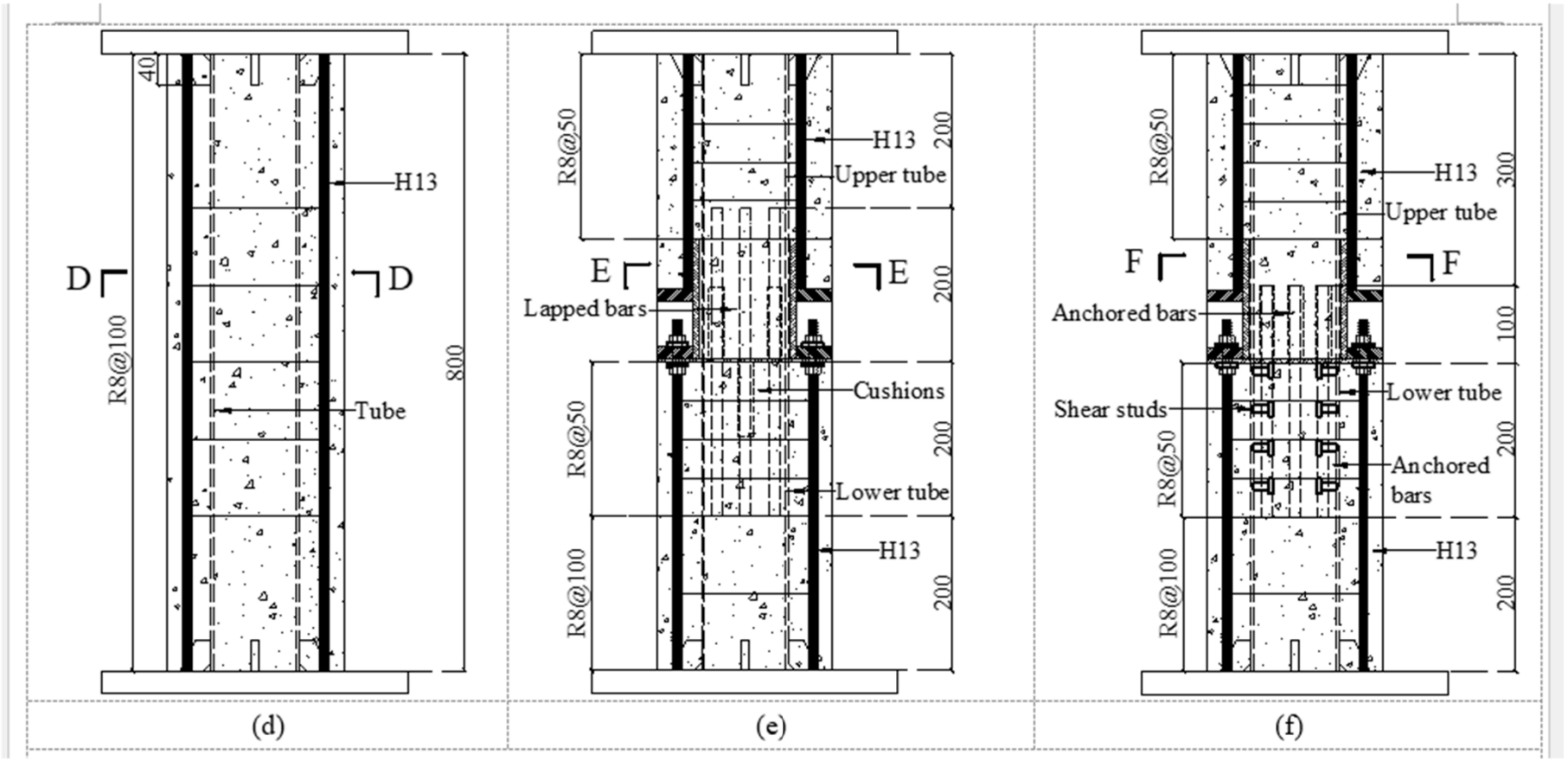

Fig. 5D **Fig. 5E** **Fig. 5F**

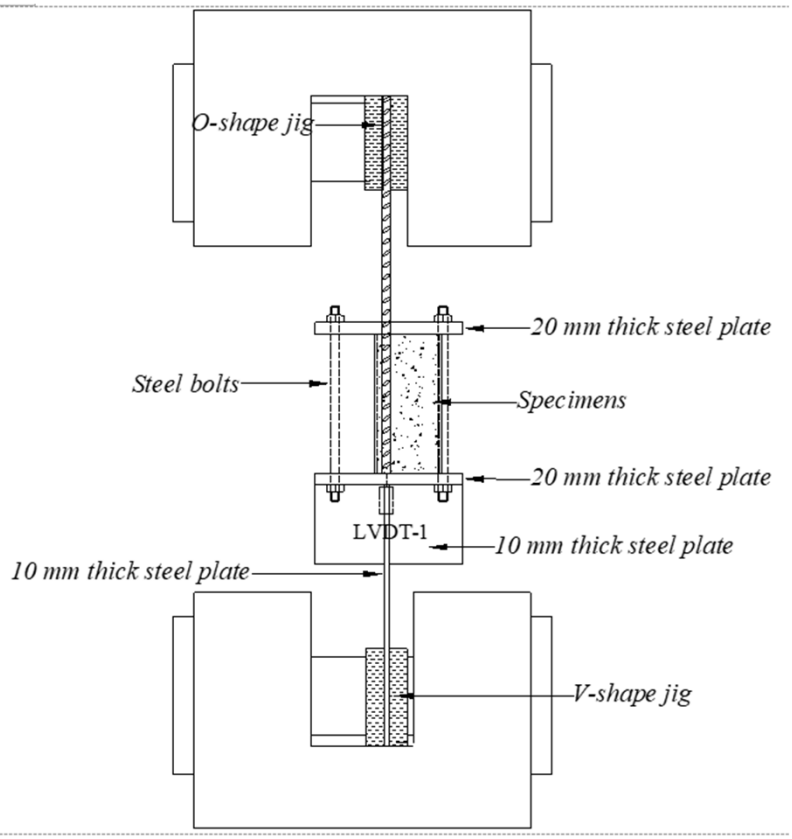

Fig. 6 Setup for pullout tests

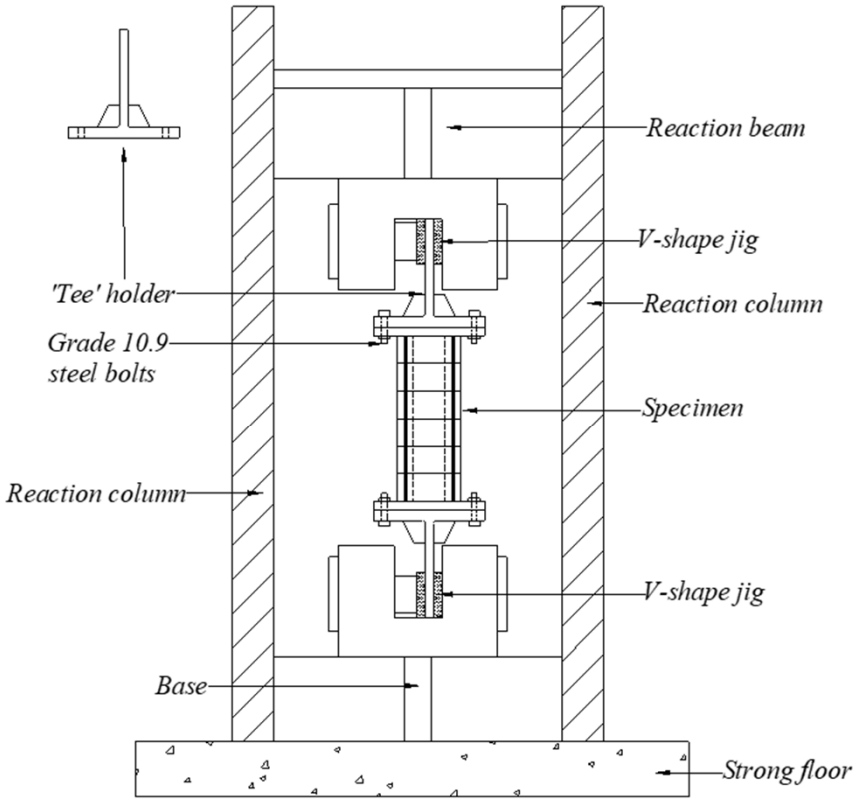

Fig. 7 Setup for connection tests

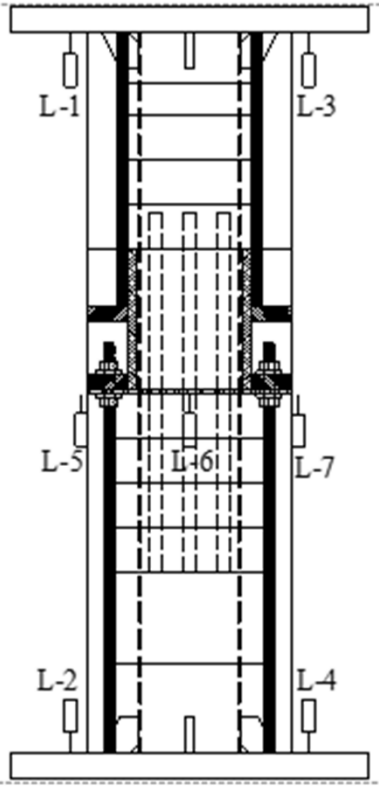

(a) Arrangement of LVDTs

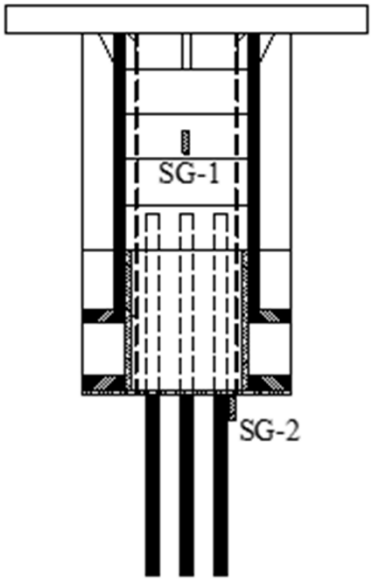

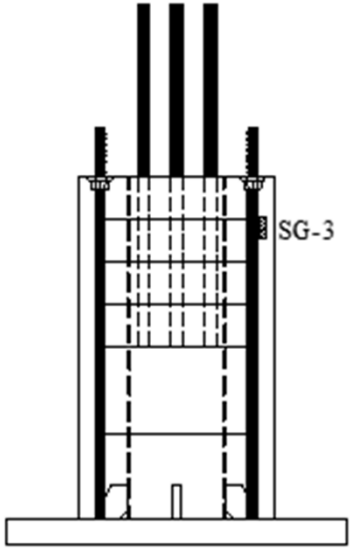

(b) Arrangement of strain gauges

Fig. 8 Measurement scheme of test specimens

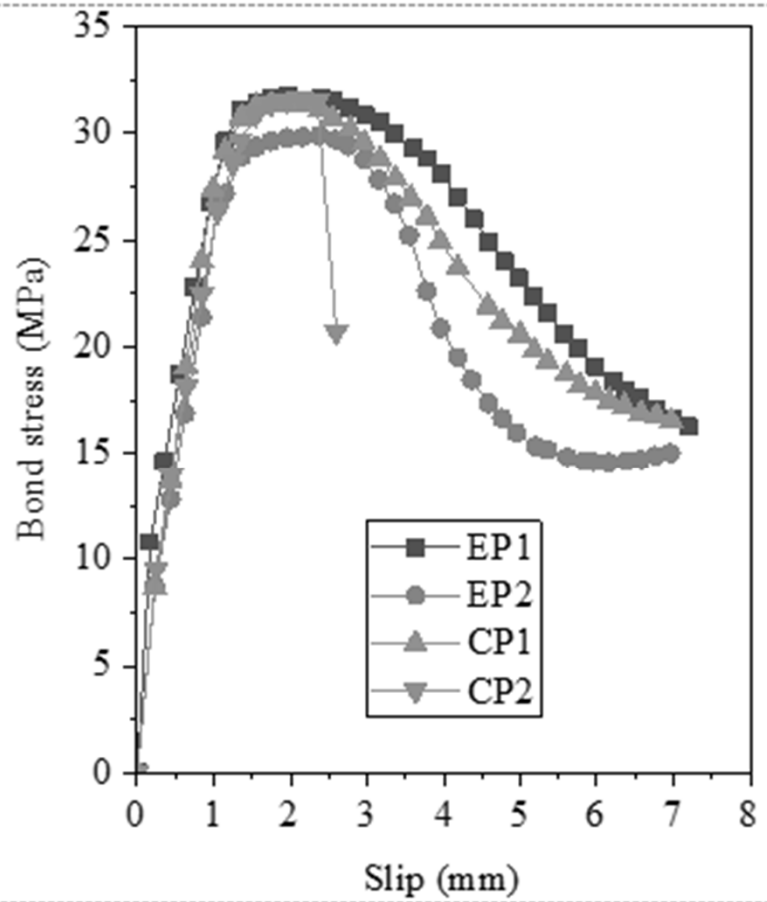

Fig. 9 Bond stress-slip relationships of pullout tests

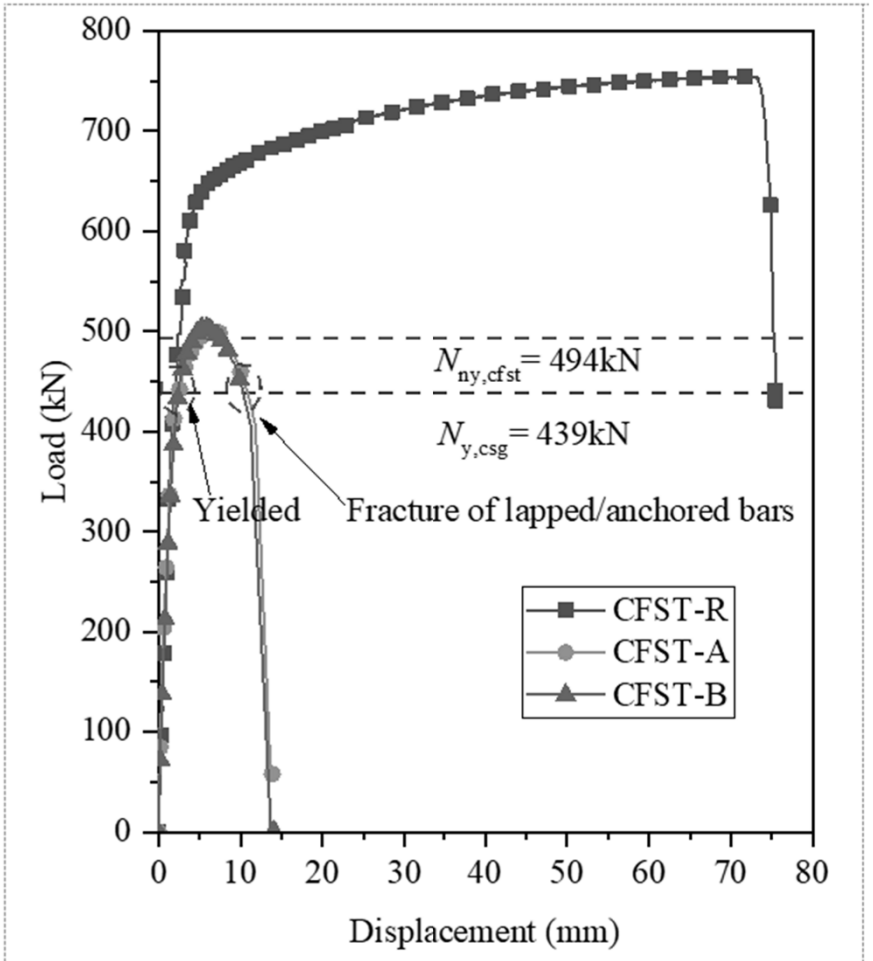

Fig. 10 Load–displacement relationships of CFST specimens

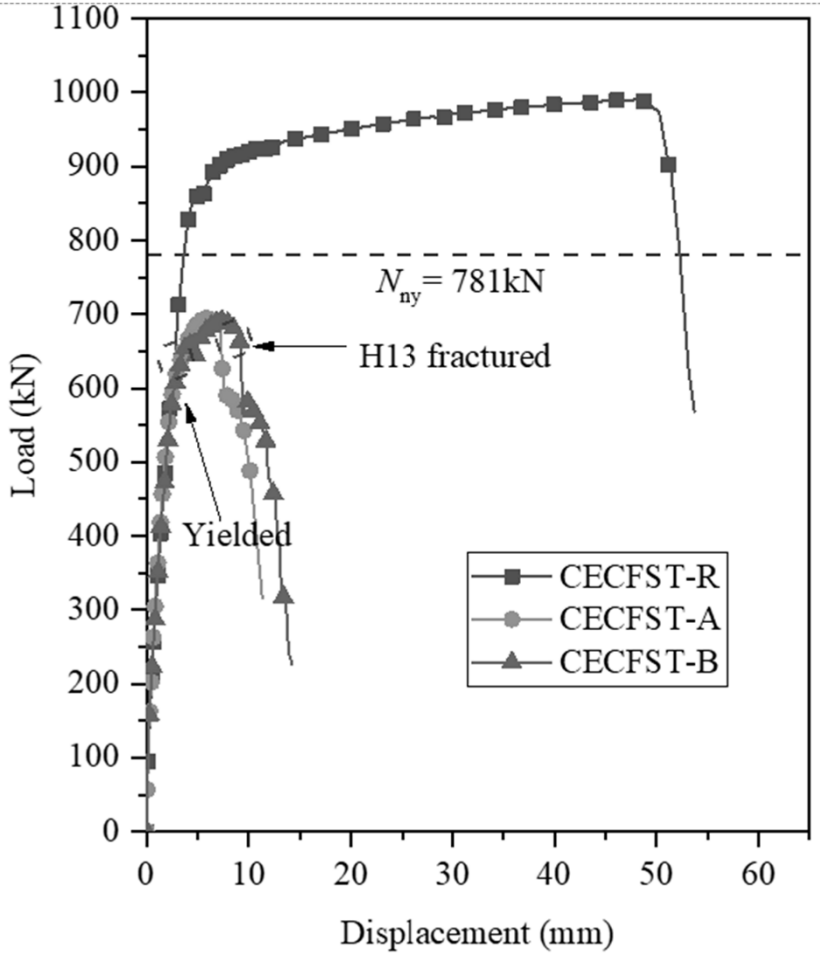

Fig. 11 Load–displacement relationship of CECFST specimens

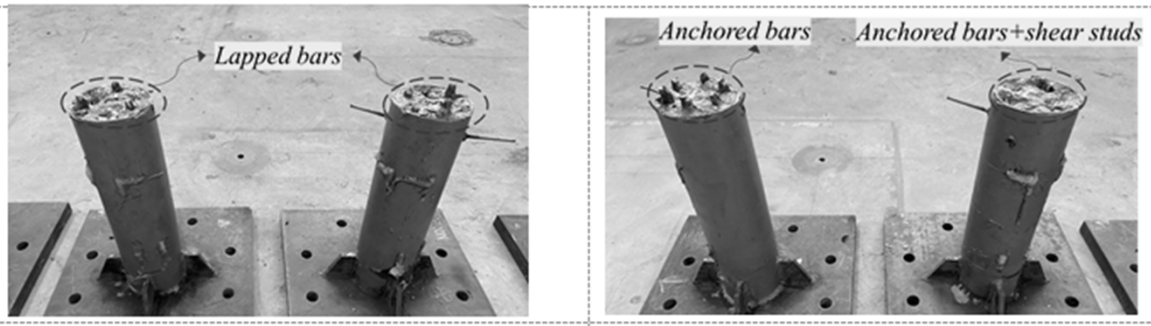

(a) CFST-A (b) CFST-B

Fig. 12 Failure modes of CFST connections

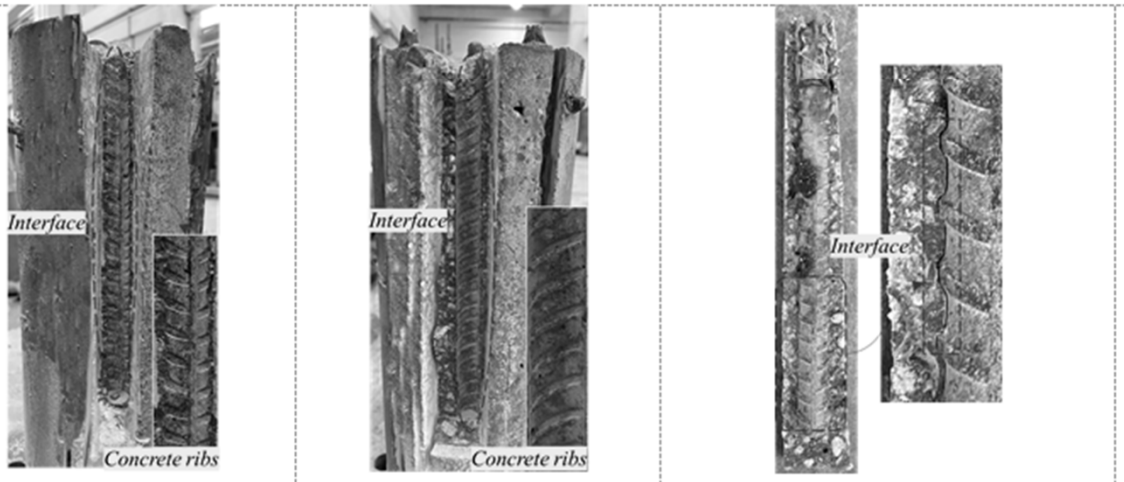

(a) Interface of CFST-A (b) Interface of CFST-B (c) Extracted Lapped bars

Fig. 13 Interfaces between reinforcing bars and inner concrete core

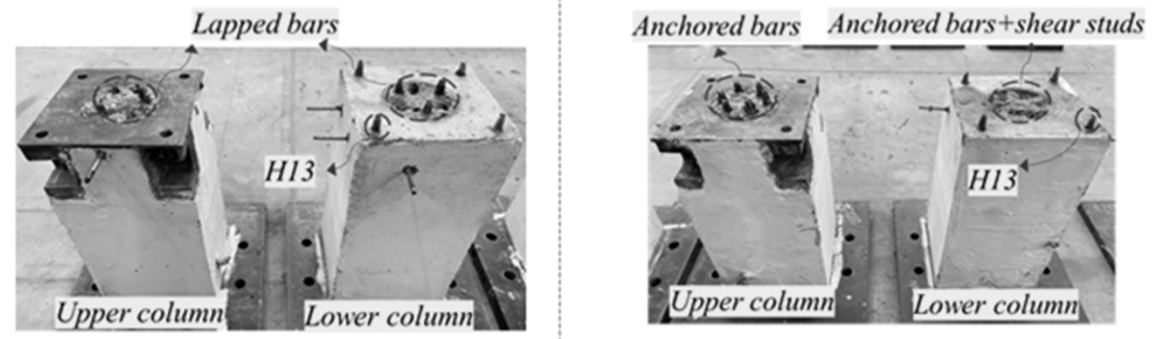

(a) Specimen CECFST-A (b) Specimen CECFST-B

Fig. 14 Failure modes of CECFST connections

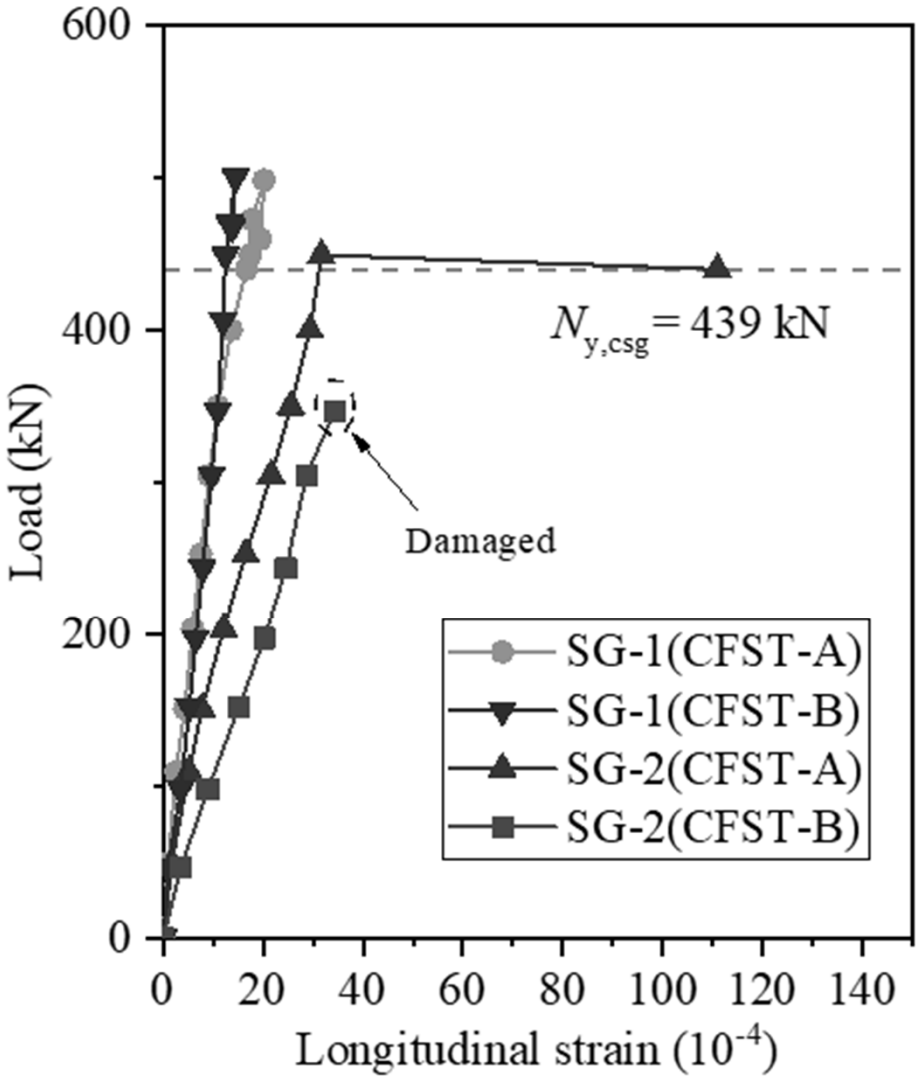

Fig. 15 Load–strain relationships of CFST connections

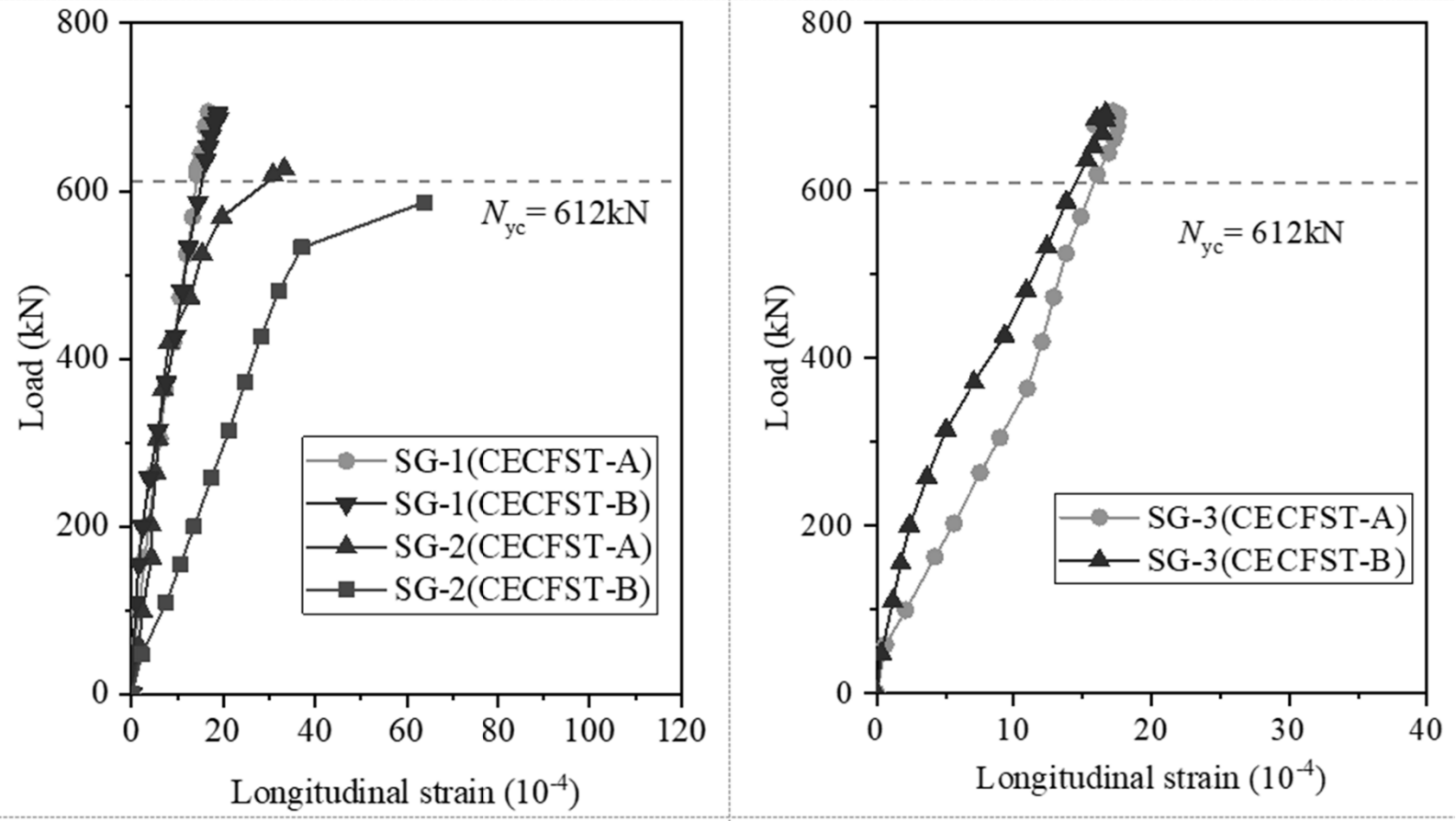

(a) Inner CFST connections (b) Outer RC connections

Fig. 16 Load–strain relationships of CECFST connections

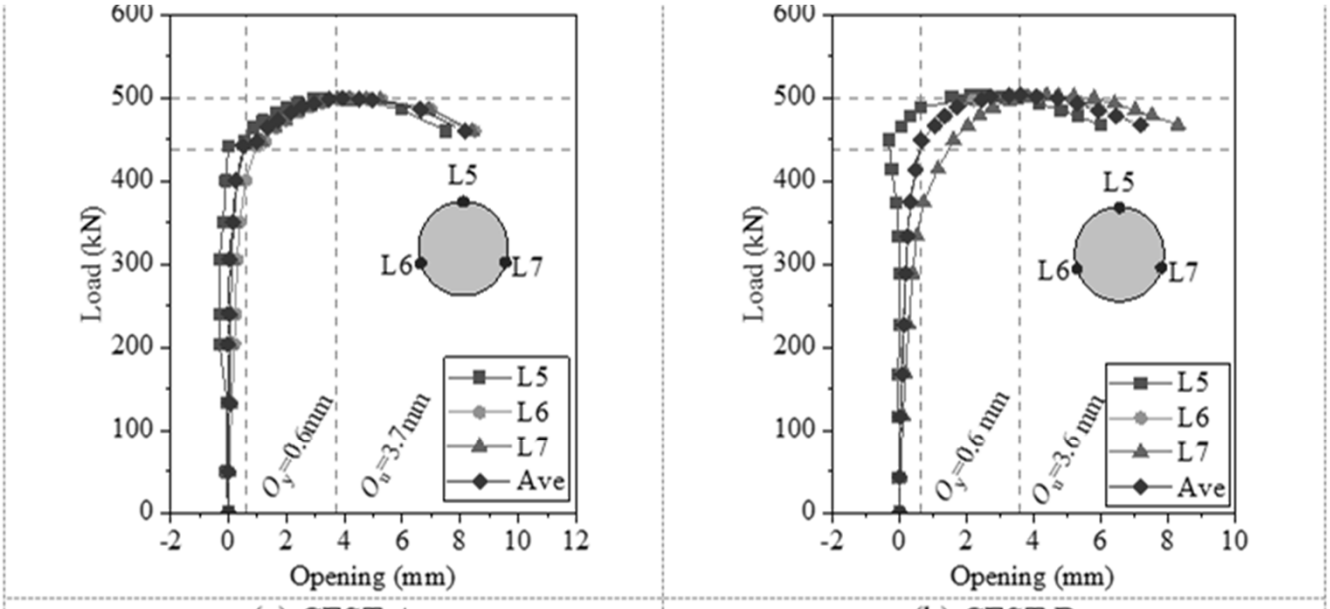

(a) CFST-A

(b) CFST-B

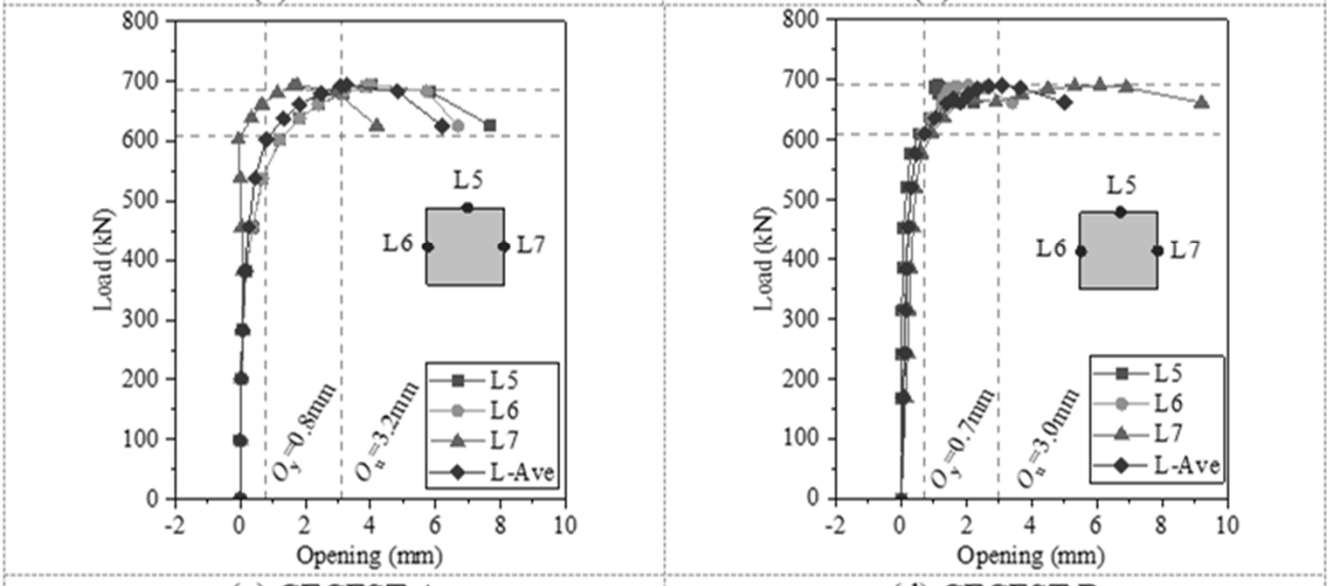

(c) CECFST-A

(d) CECFST-B

Fig. 17 Load–opening relationships of four connection specimens

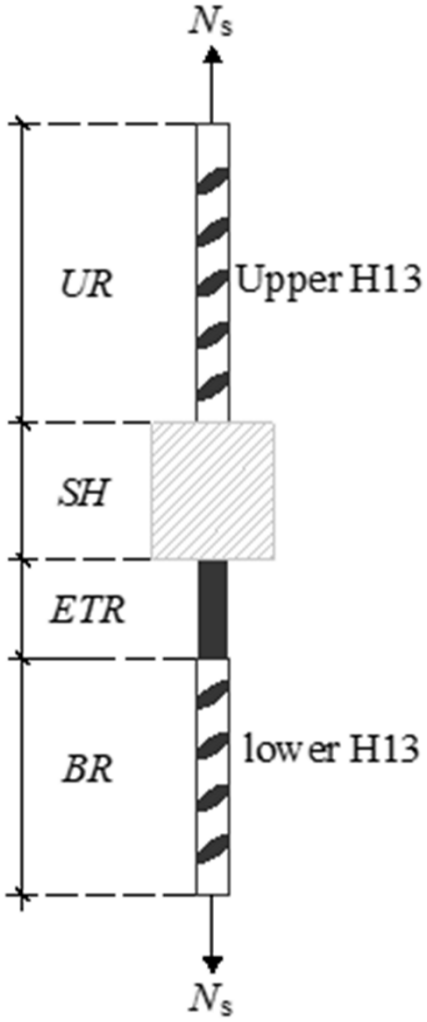

Outer RC connection

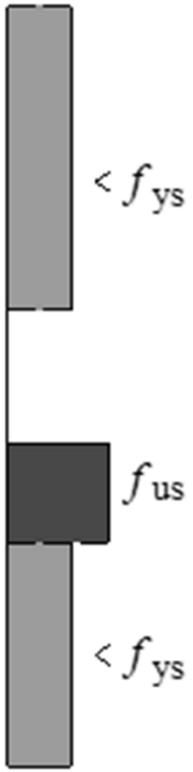

Stress

Strain

Fig. 18 Stress and strain distribution of the RC connection at ultimate state

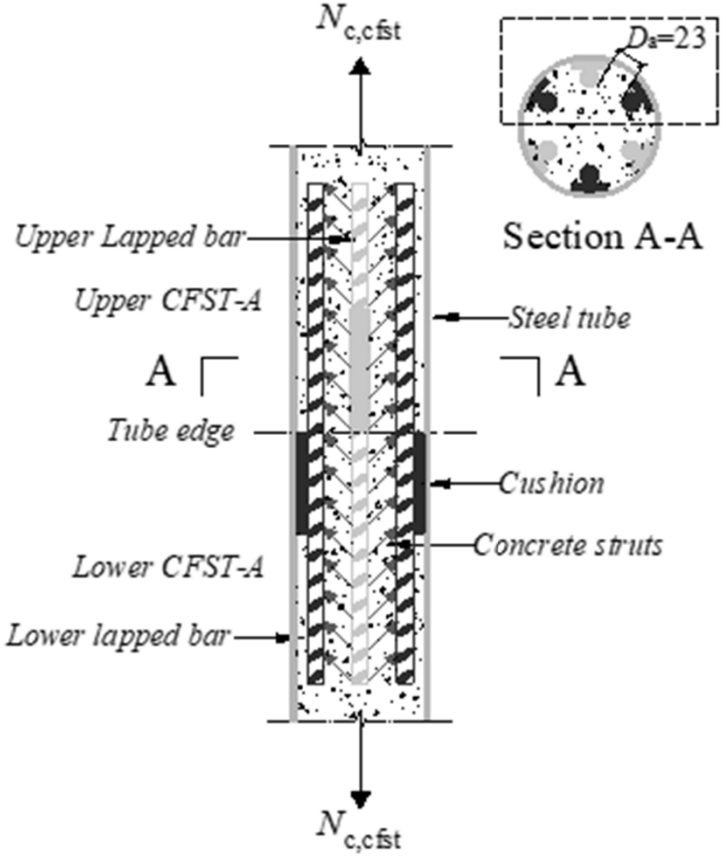

(a) PCDC-A

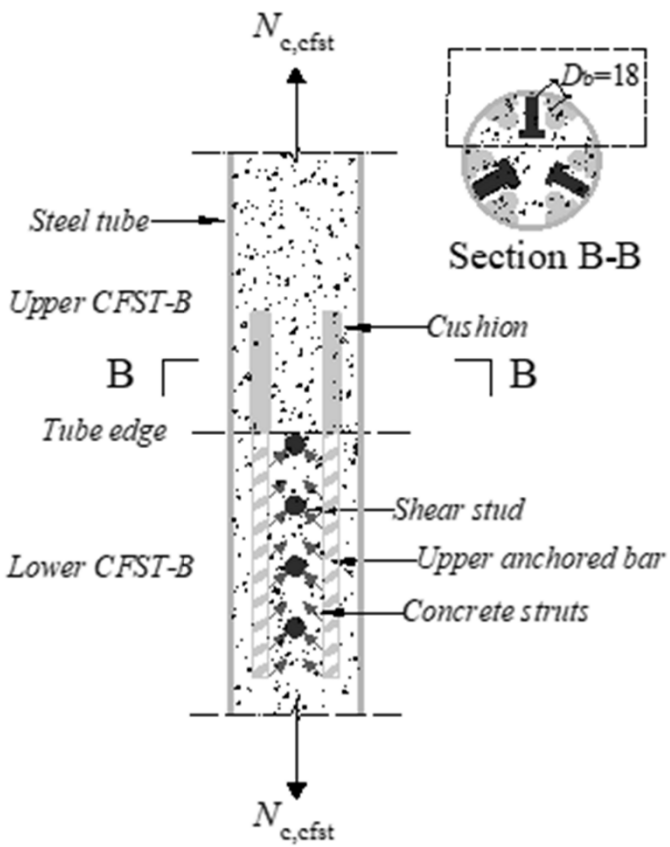

(b) PCDC-B

Fig. 19 Load transfer mechanism of CFST connections

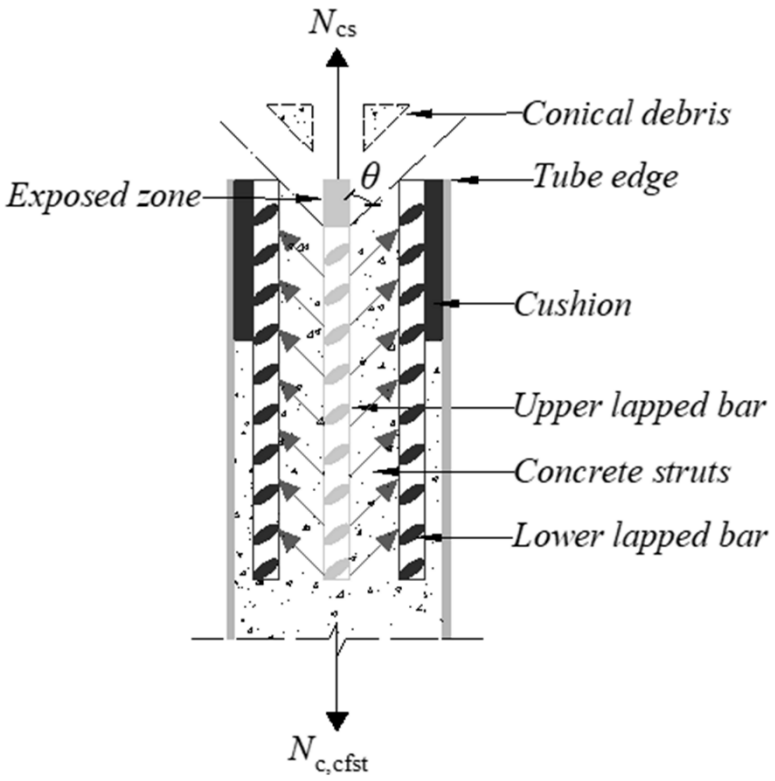

(a) Proposed mechanism

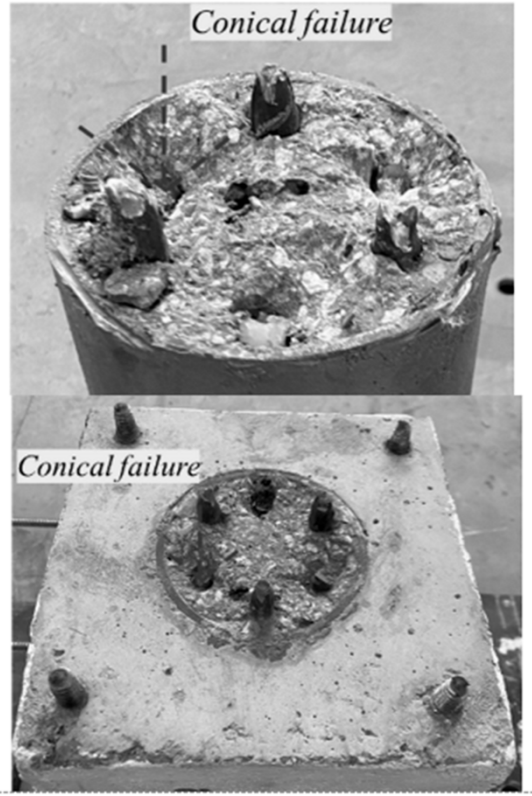

(b) Experimental result

Fig. 20 Failure mechanism of inner CFST connection of PCDC-A

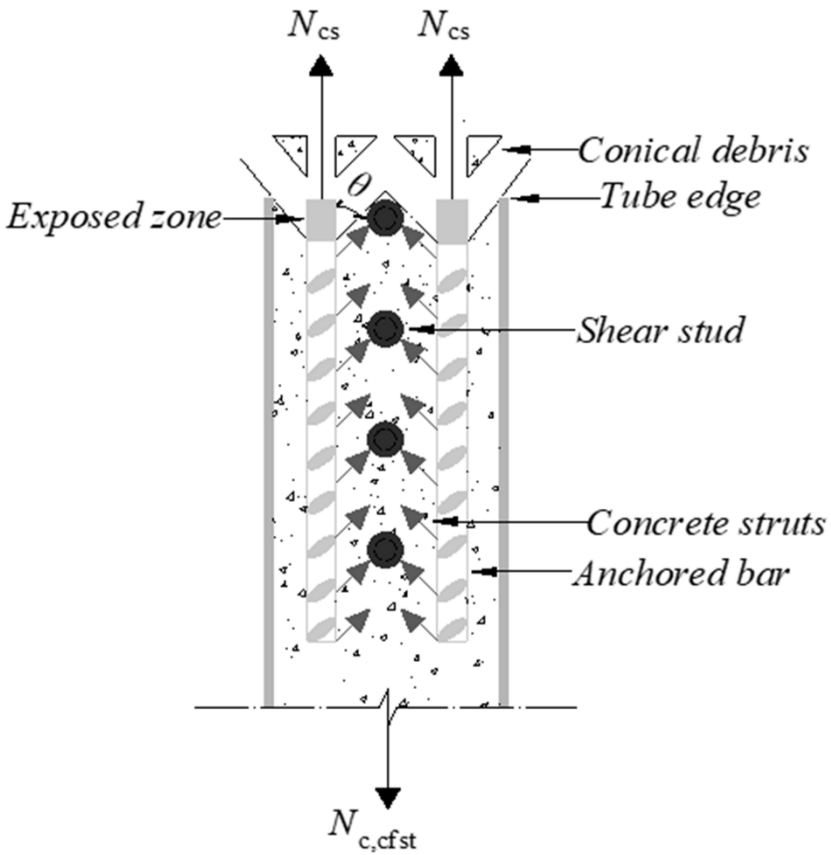

(a) Proposed mechanism

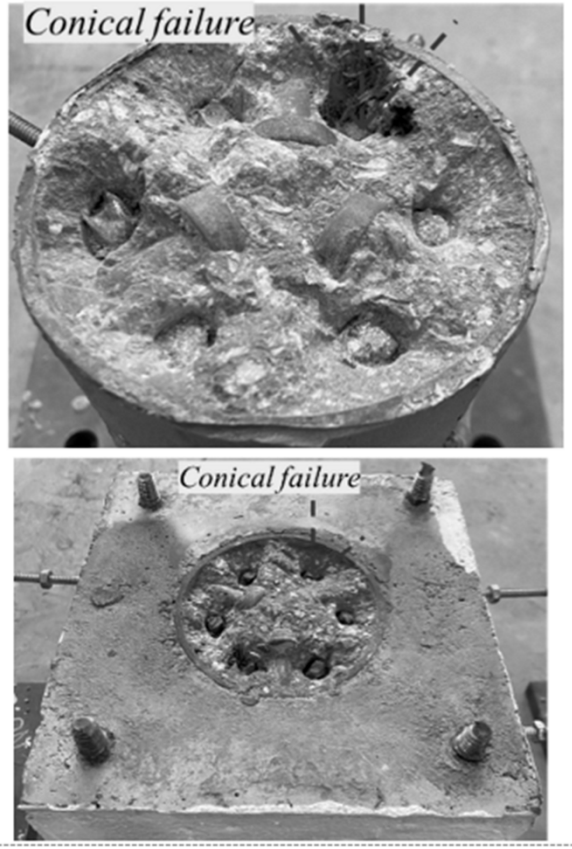

(b) Experimental result

Fig. 21 Failure mechanism of inner CFST connection of PCDC-B

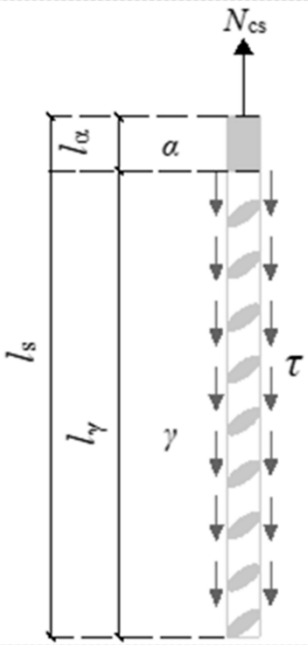

(a) Lapped/anchored bars

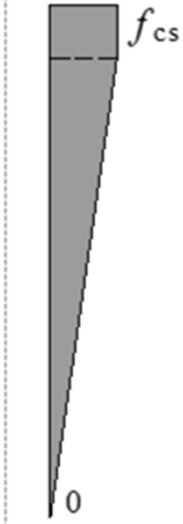

(b) Stress

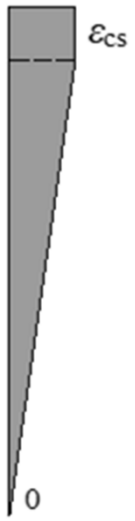

(c) Strain

Fig. 22 Stress and strain distributions of lapped /anchored bars at elastic stage ($N_{c,cfst} \leqslant N_{y,csg}$)

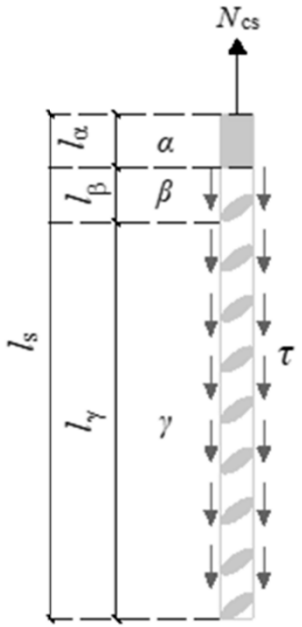

(a) Lapped/anchored bars

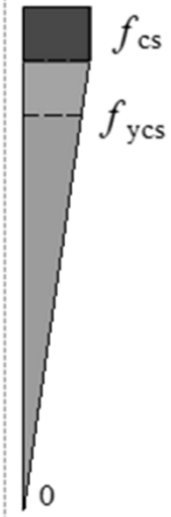

(b) Stress

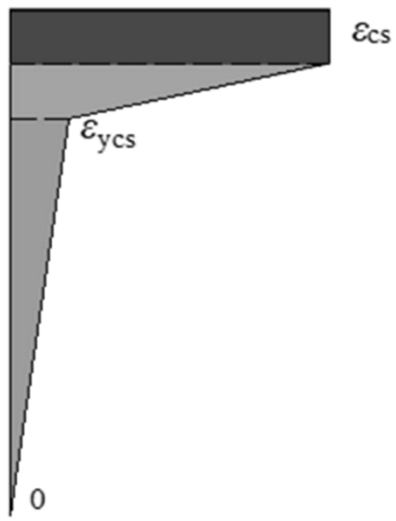

(c) Strain

Fig. 23 Stress and train distributions of lapped/anchored bars at plastic stage ($N_{c,cfst} > N_{y,csg}$)

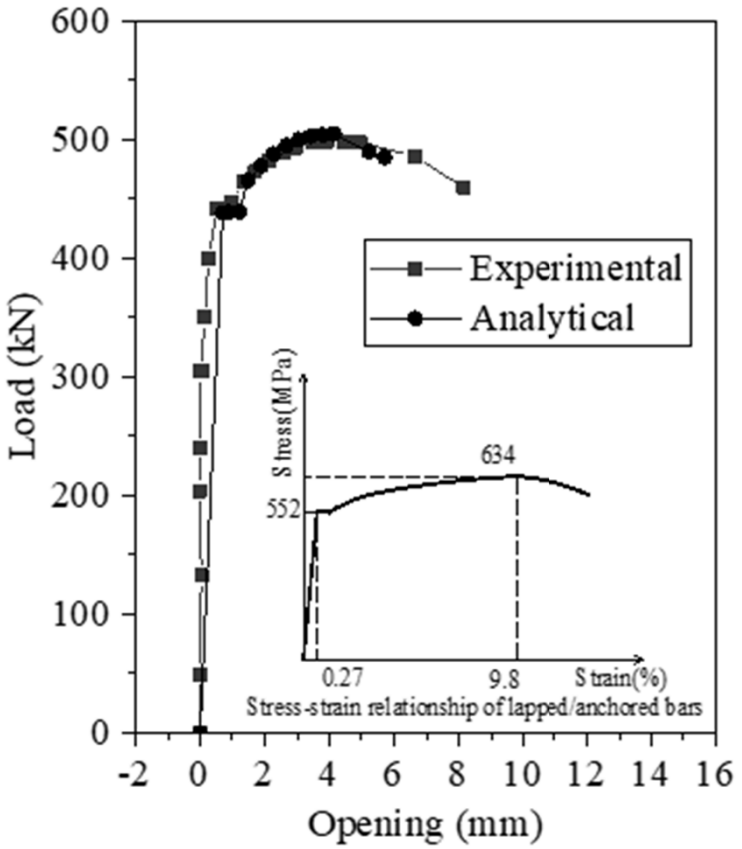

a) CFST-A

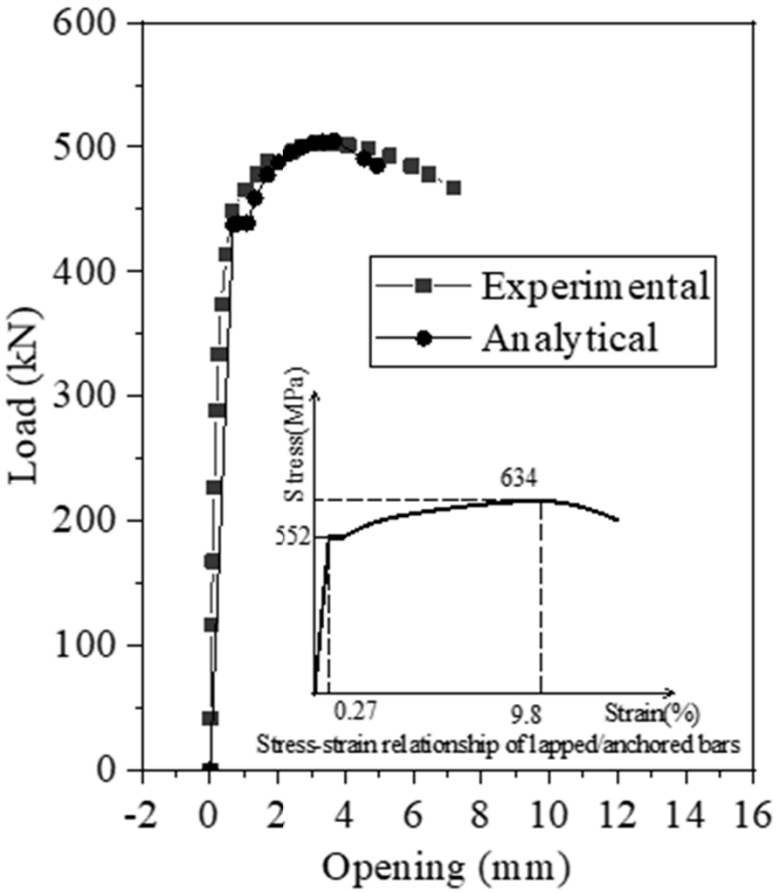

b) CFST-B

Fig. 24 Predication of load–opening relationships of CFST connections

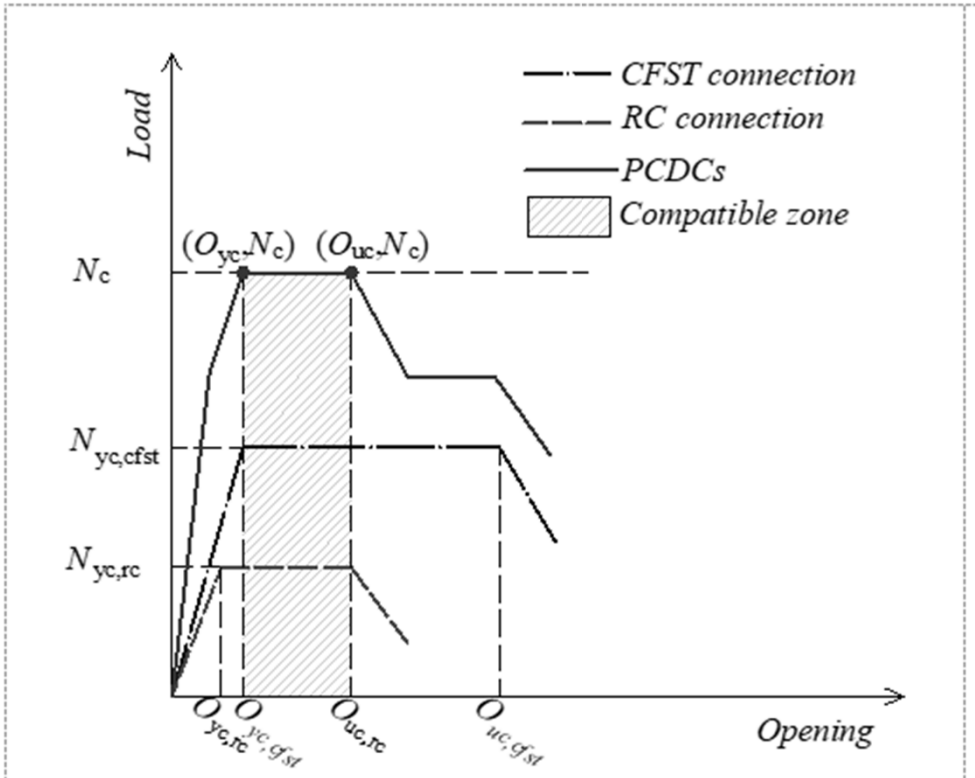

Fig. 25 Compatibility analysis of connection opening

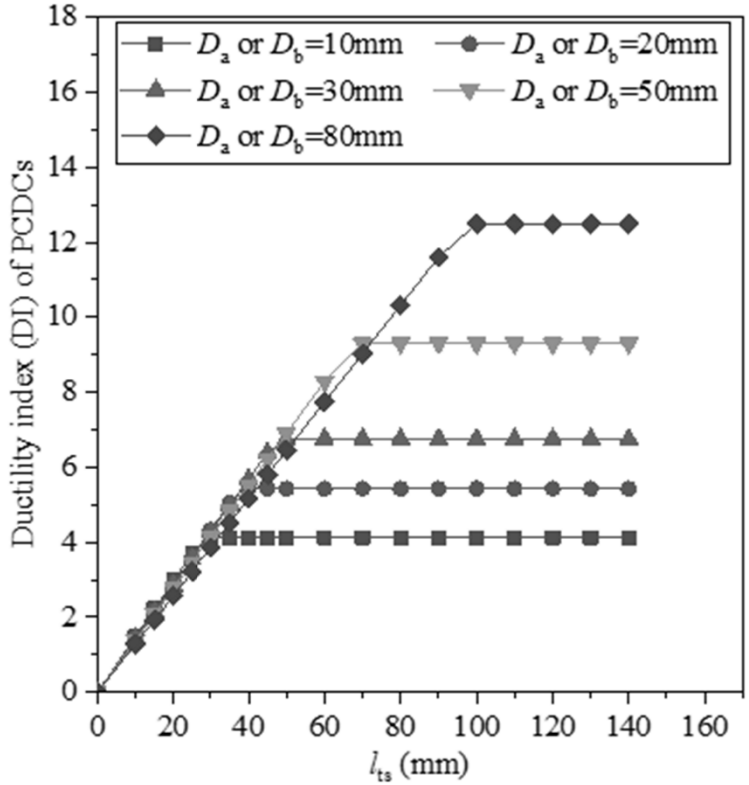

Fig. 26 Parametric study on the ductility of PCDCs

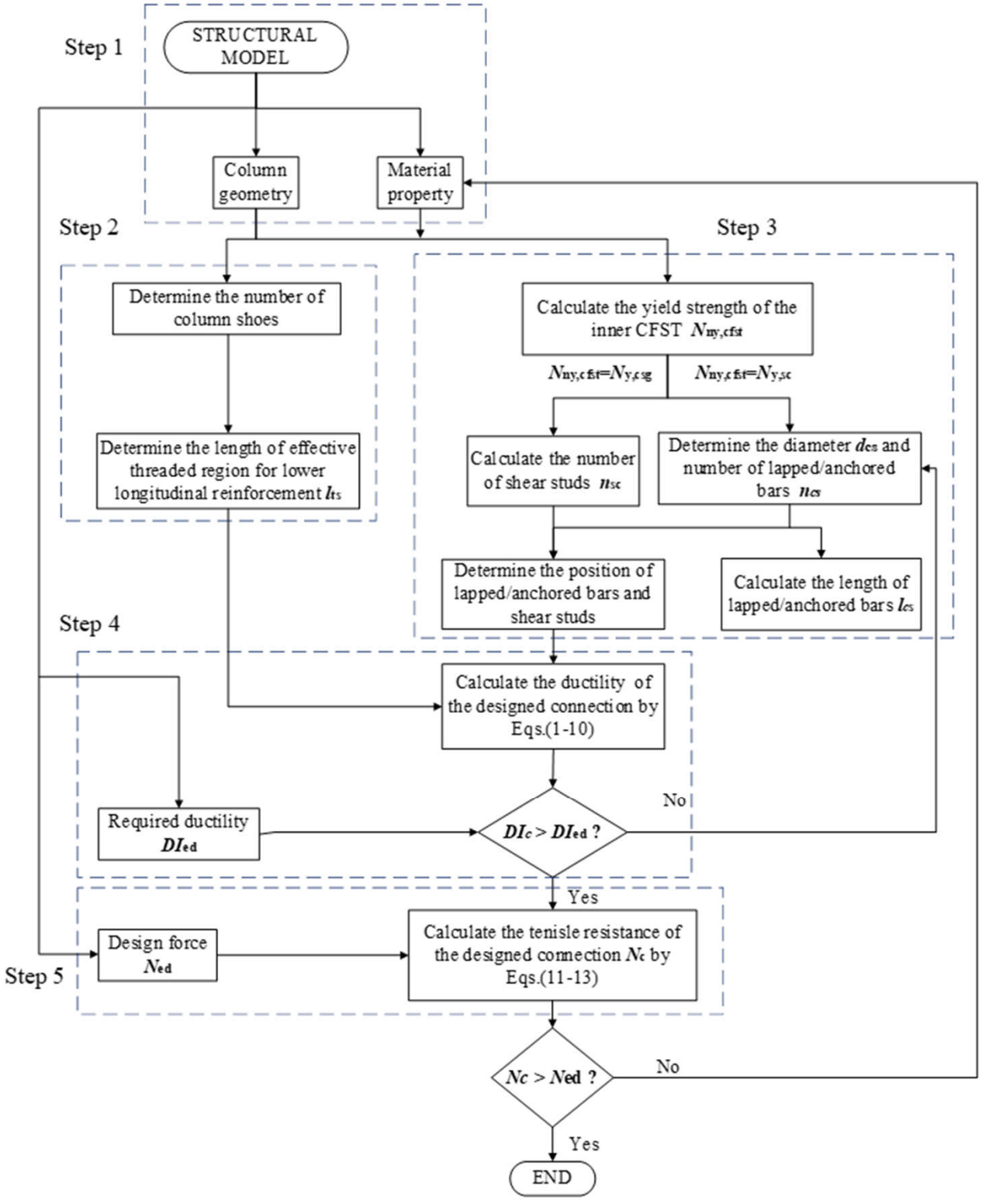
Step 1
STRUCTURAL MODEL
Column geometry
Material property
Step 2
Step 3
Determine the number of column shoes
Calculate the yield strength of the inner CFST $N_{ny,cfst}$
$N_{ny,cfst}=N_{y,csg}$
$N_{ny,cfst}=N_{y,sc}$
Determine the length of effective threaded region for lower longitudinal reinforcement l_{ts}
Calculate the number of shear studs n_{sc}
Determine the diameter d_{cs} and number of lapped/anchored bars n_{cs}
Determine the position of lapped/anchored bars and shear studs
Calculate the length of lapped/anchored bars l_{cs}
Step 4
Calculate the ductility of the designed connection by Eqs.(1-10)
Required ductility DI_{ed}
$DI_c > DI_{ed}$?
No
Yes
Step 5
Design force N_{ed}
Calculate the tenisle resistance of the designed connection N_c by Eqs.(11-13)
$N_c > N_{ed}$?
No
Yes
END

Fig. 27

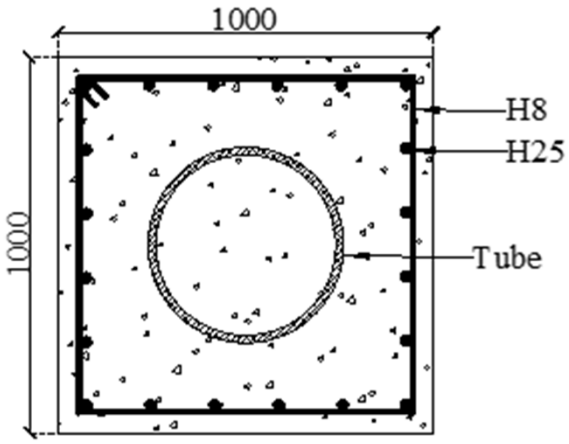

Fig. 28 Cross-section of CECFST columns

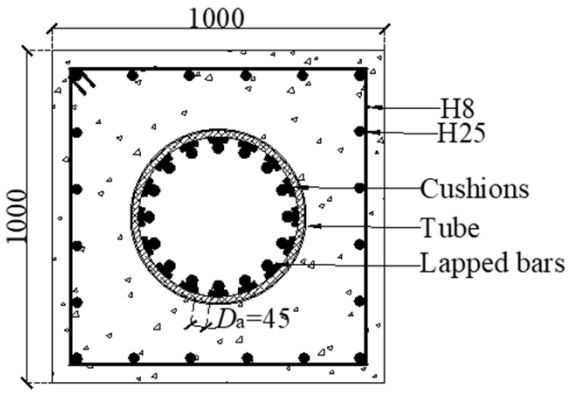

(a) PCDC-A

Fig. 29

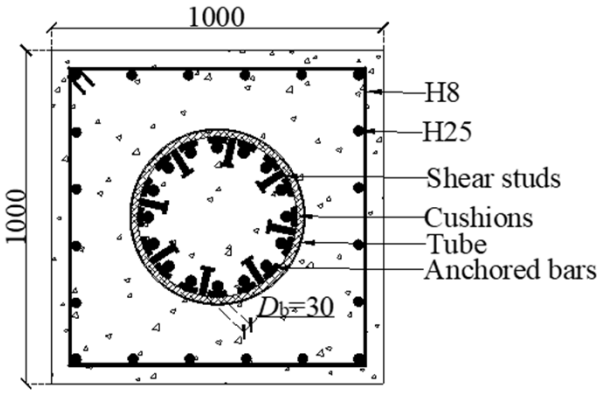

(b) PCDC-B

Fig. 30

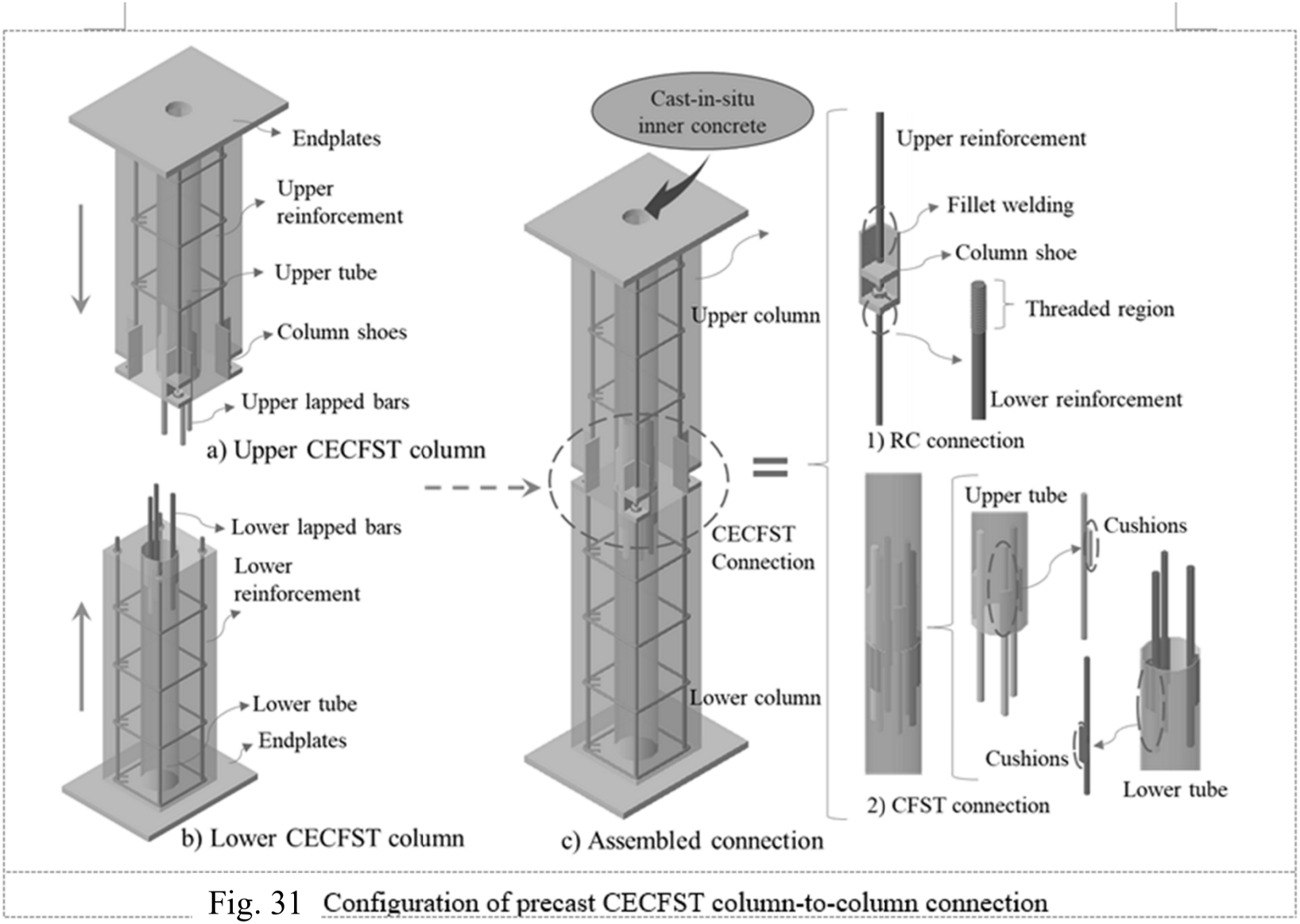

Fig. 31 Configuration of precast CECFST column-to-column connection

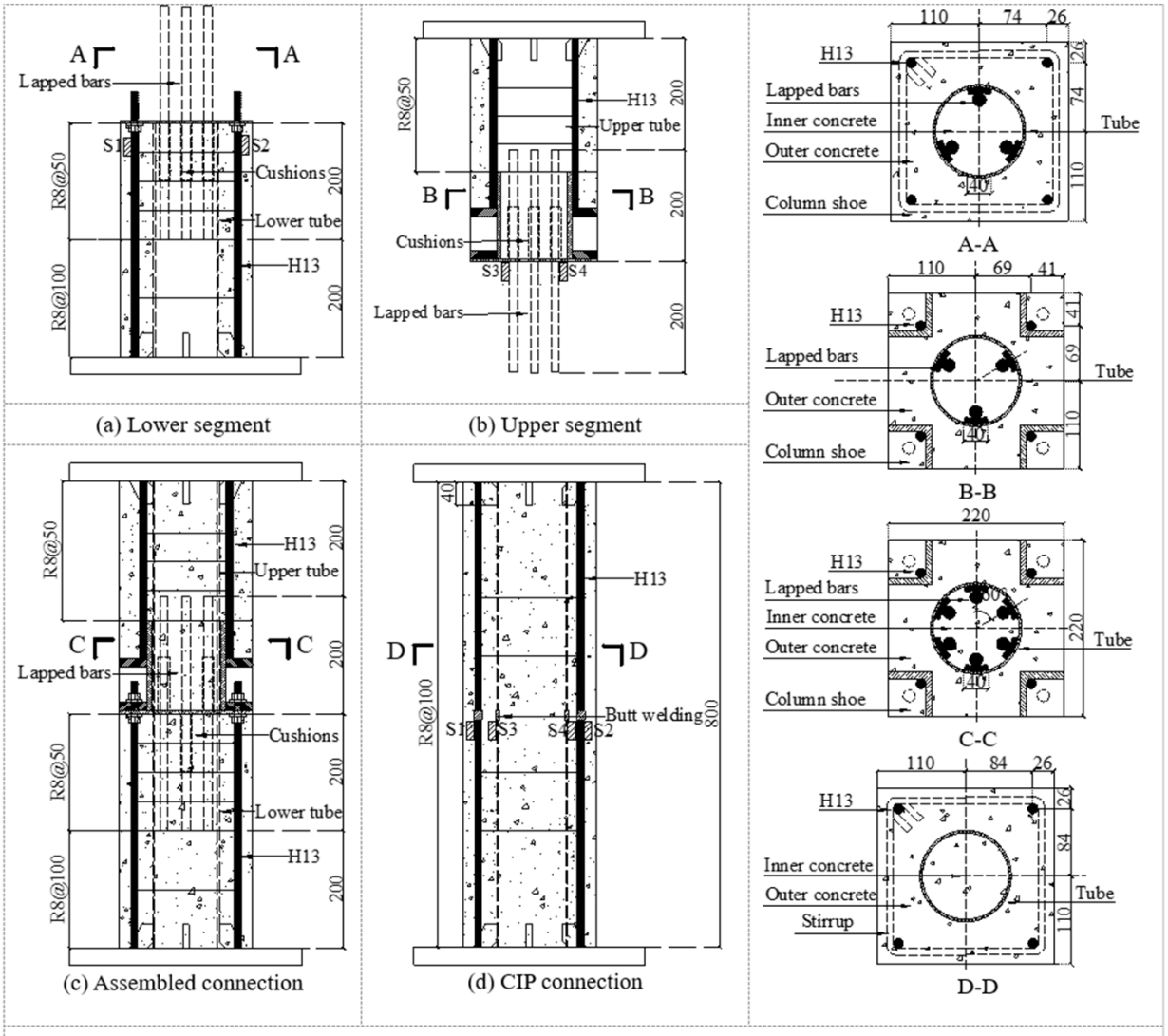

Fig. 2 Dimensions of test specimens

Fig. 32

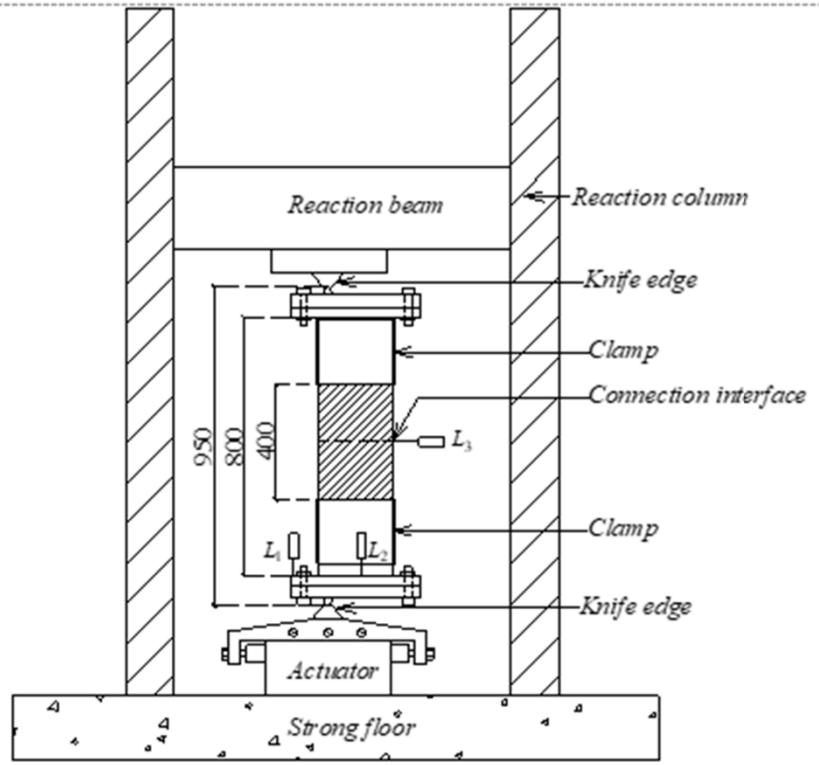

(a) Schematic setup

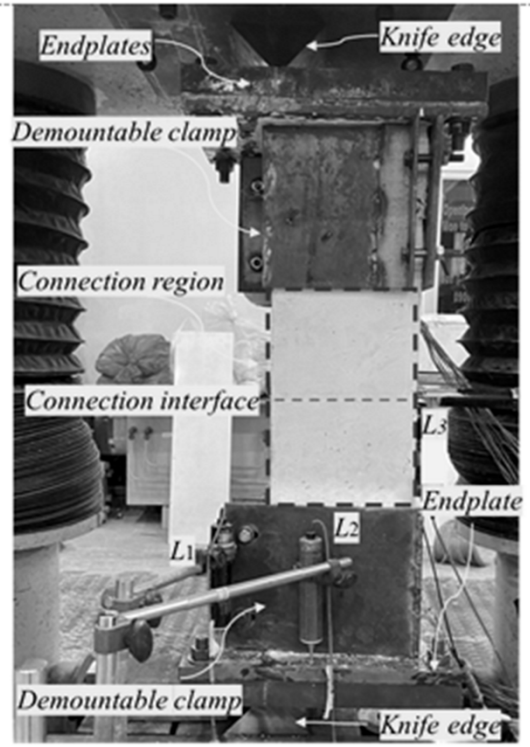

(b) Experimental setup

Test setup and instrumentation

Fig. 33

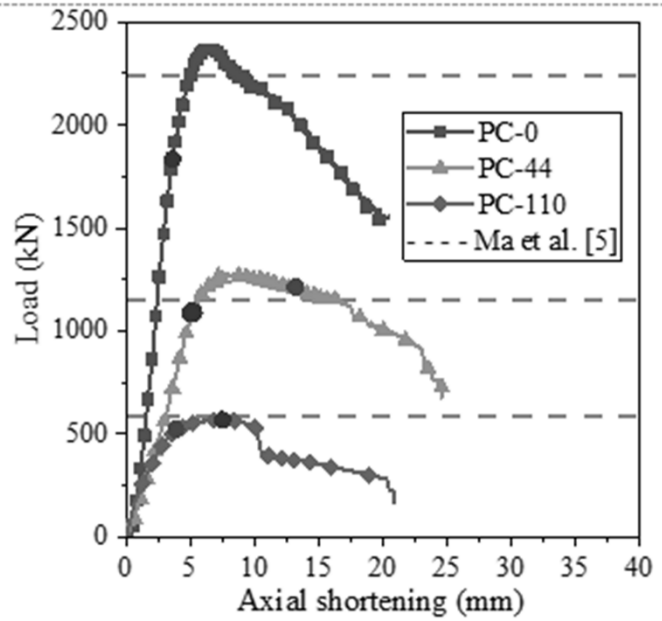

(a) No.1-No.3

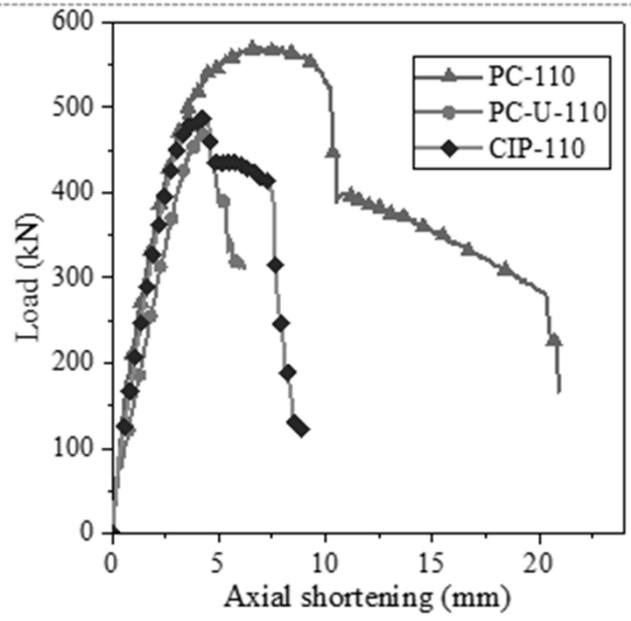

(b) No.3-No.5

Fig. 34 Load-axial shortening relationships of test specimens

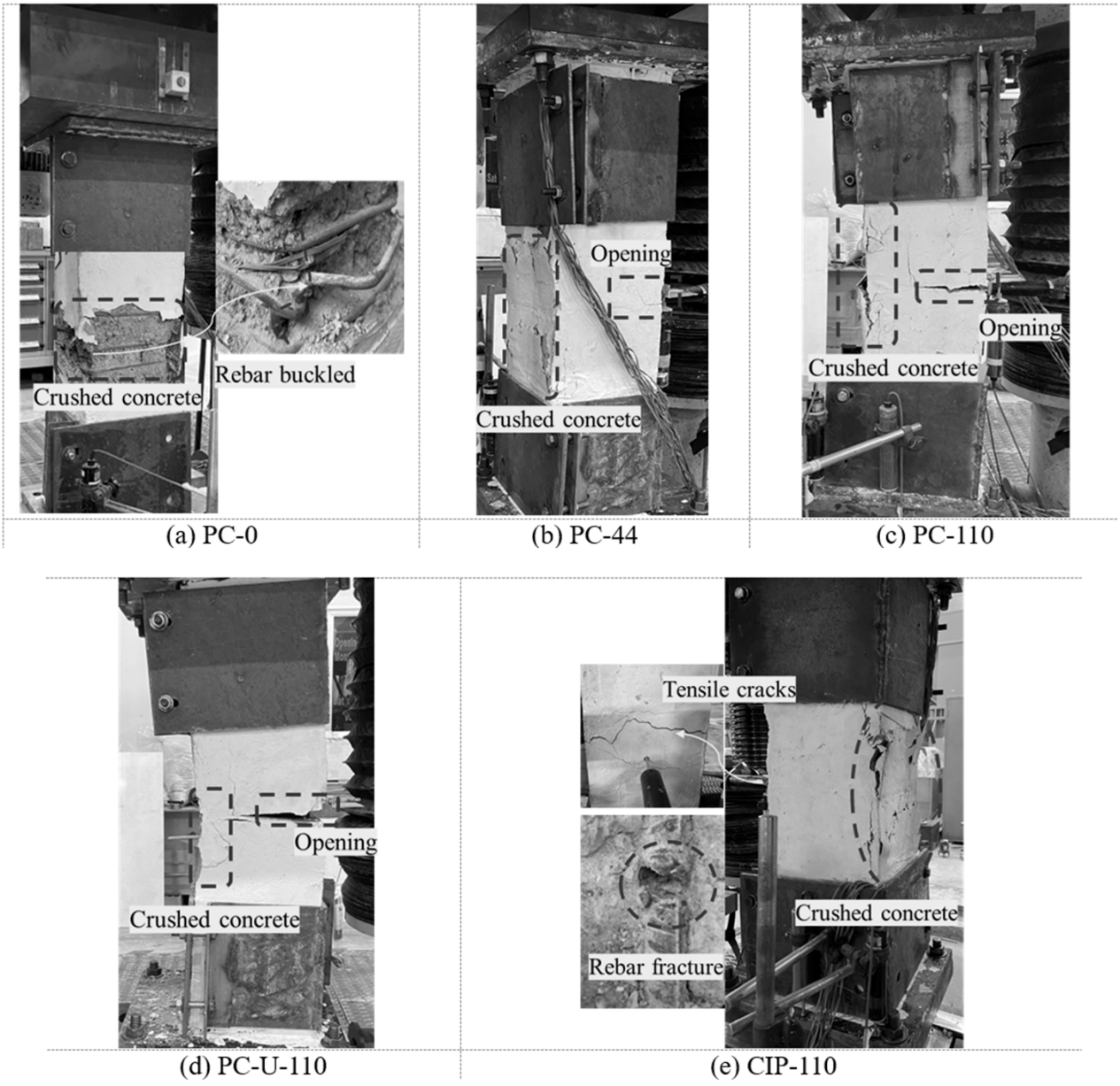

Failure modes of test specimens

Fig. 35

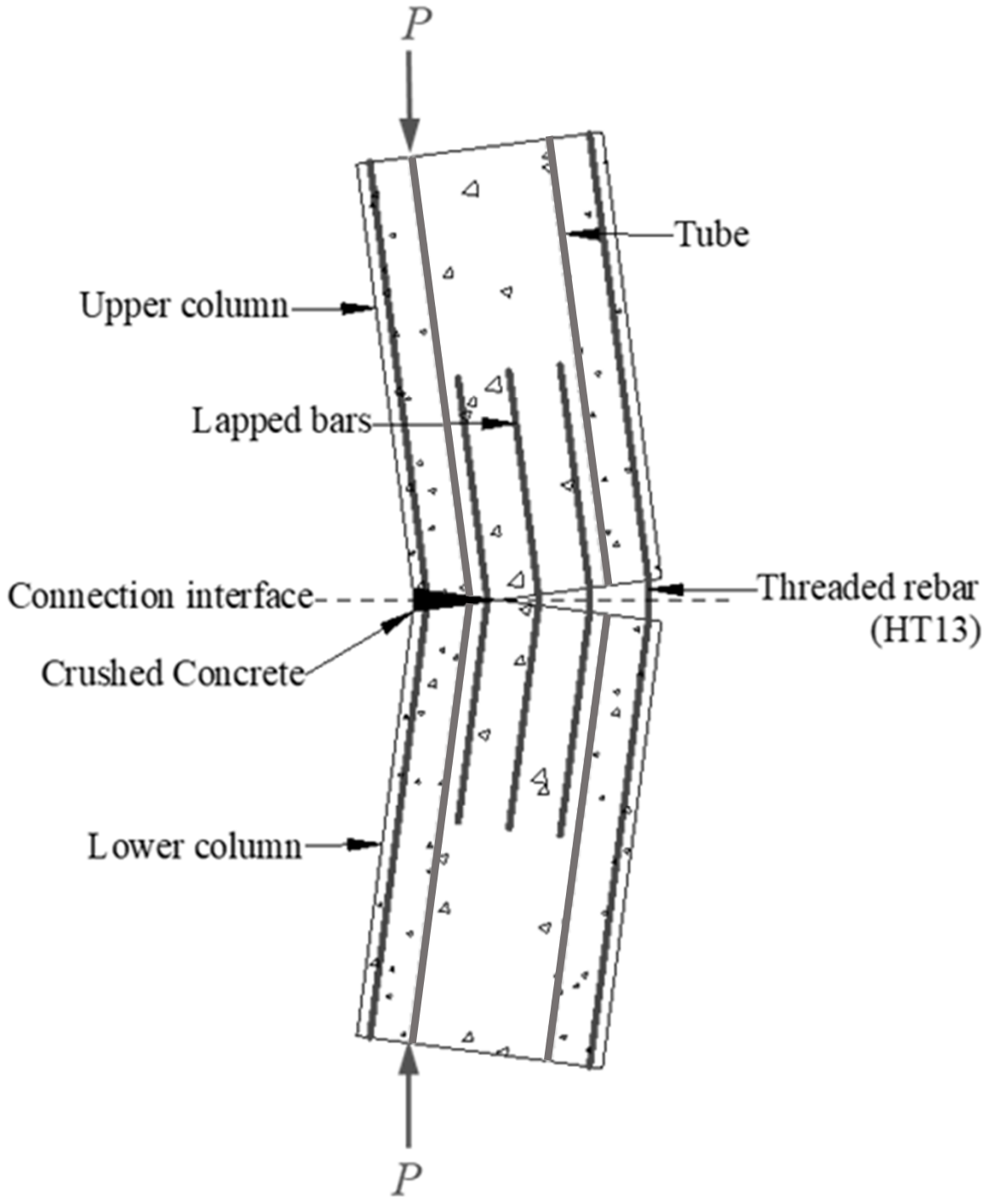

Failure mechanism of precast CECFST column-to-column connection

Fig. 36

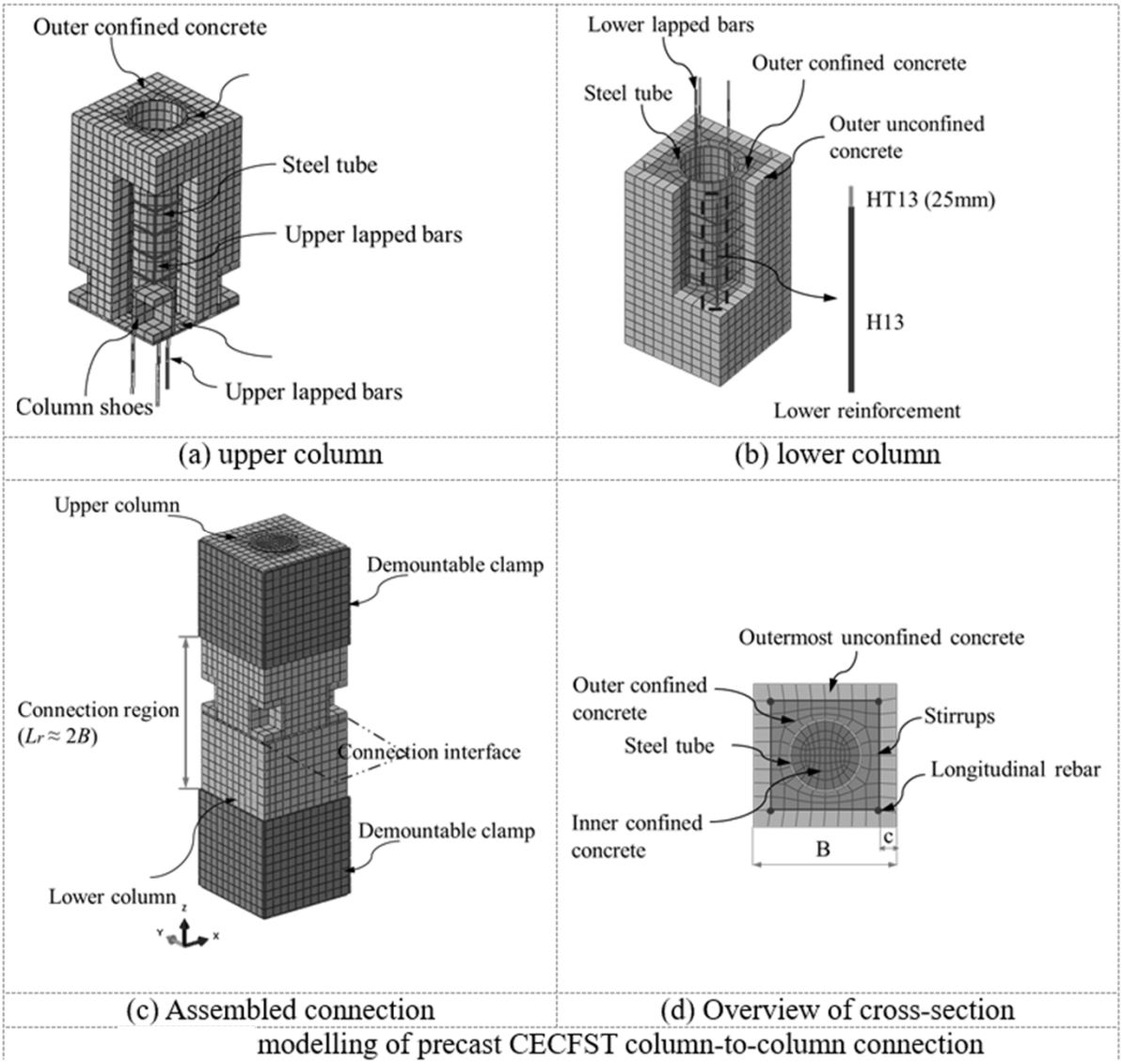

modelling of precast CECFST column-to-column connection

Fig. 37

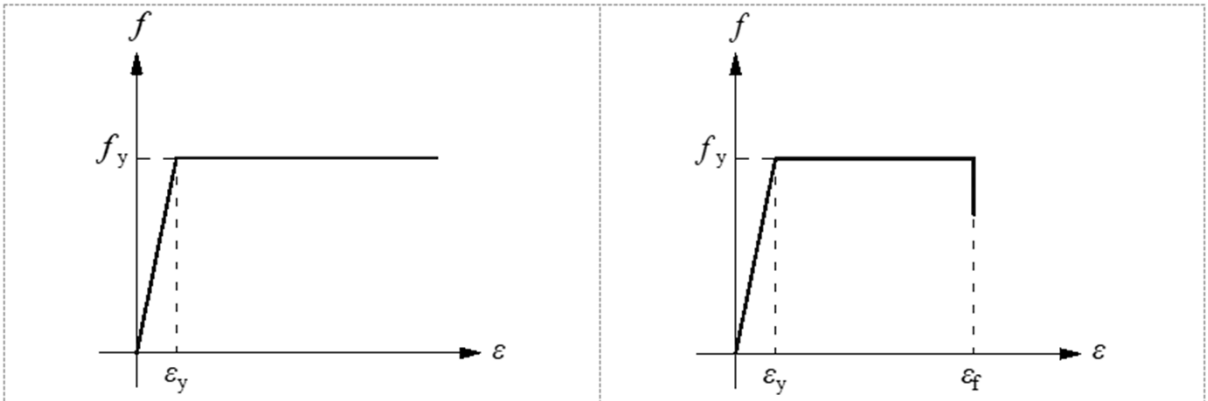

Stress-strain models used for steel components

Fig. 38

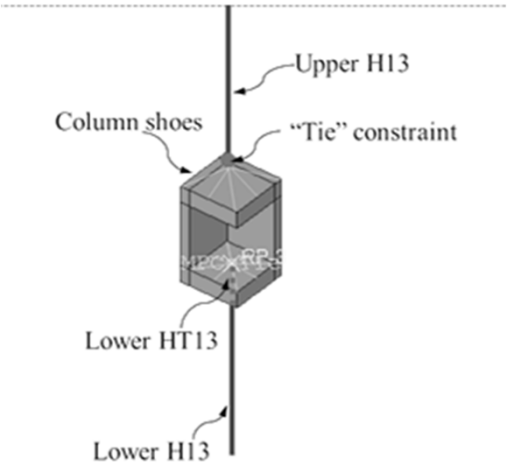

Fig. 9 Modelling of RC connection

Fig. 39

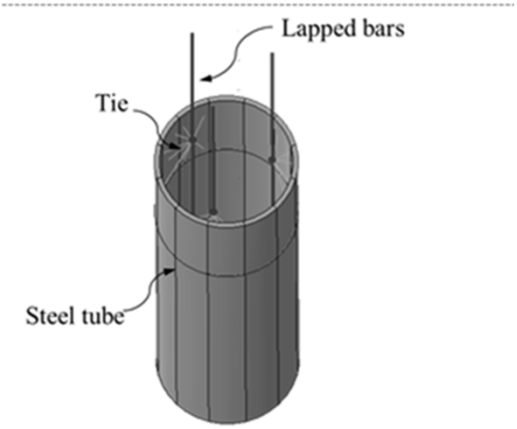

10 Modelling of CFST connection

Fig. 40

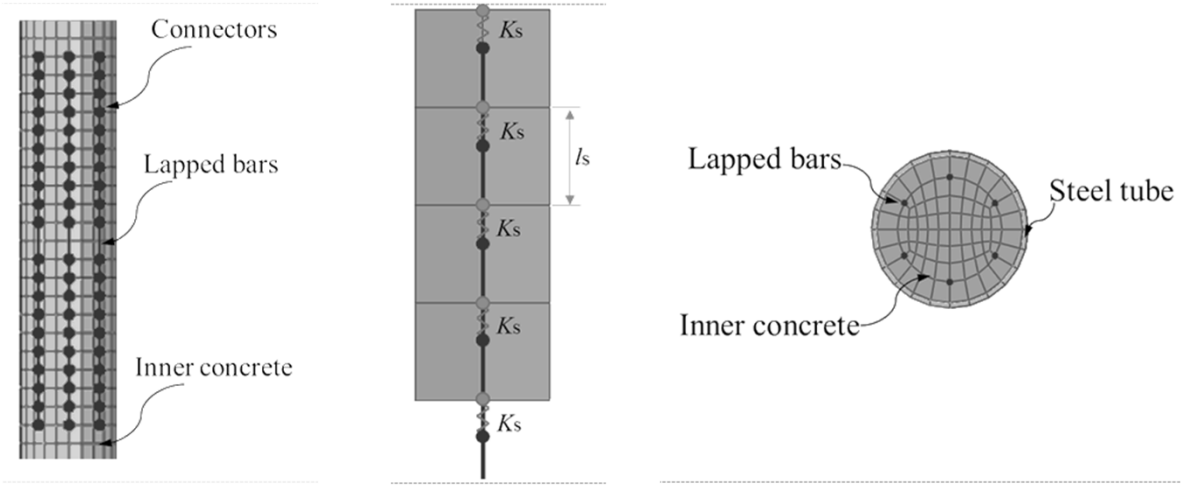

Modelling of bond-slip behaviour of lapped bars

Fig. 41

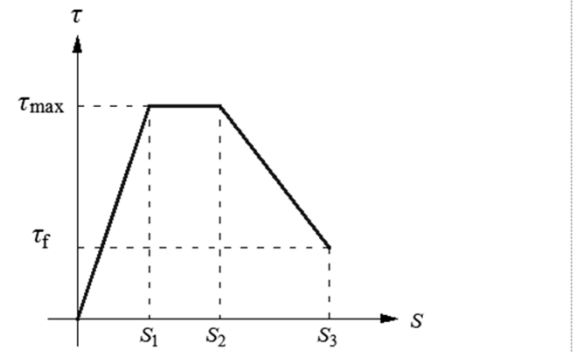

Codified bond-slip relationship (FIB Code)

Fig. 42

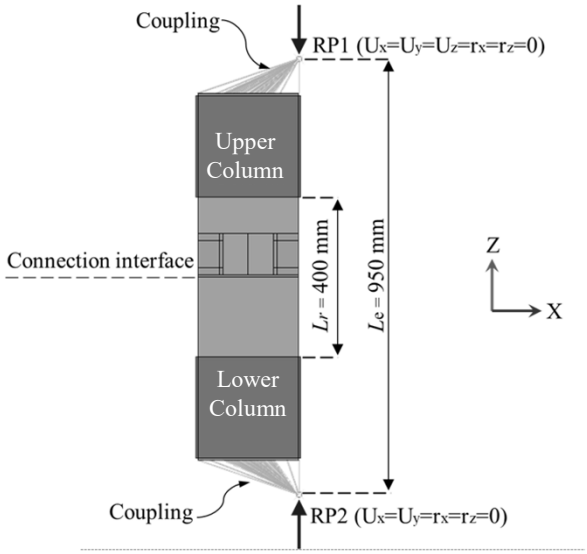

Boundary conditions of the test specimens

Fig. 43

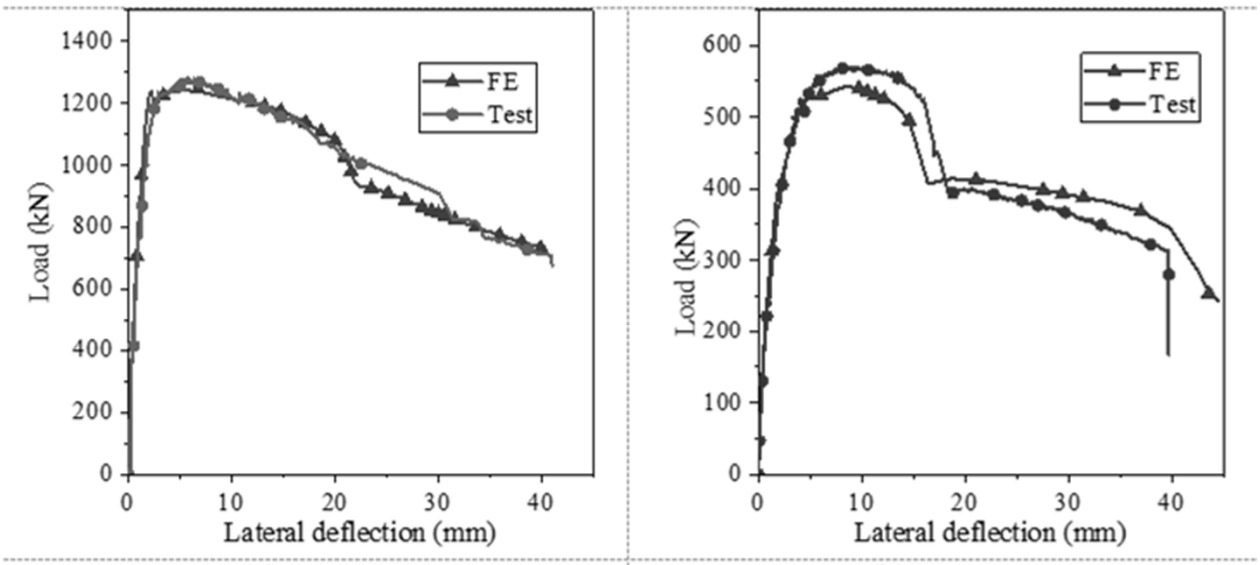

Prediction of load-lateral deflection relationships

Fig. 44

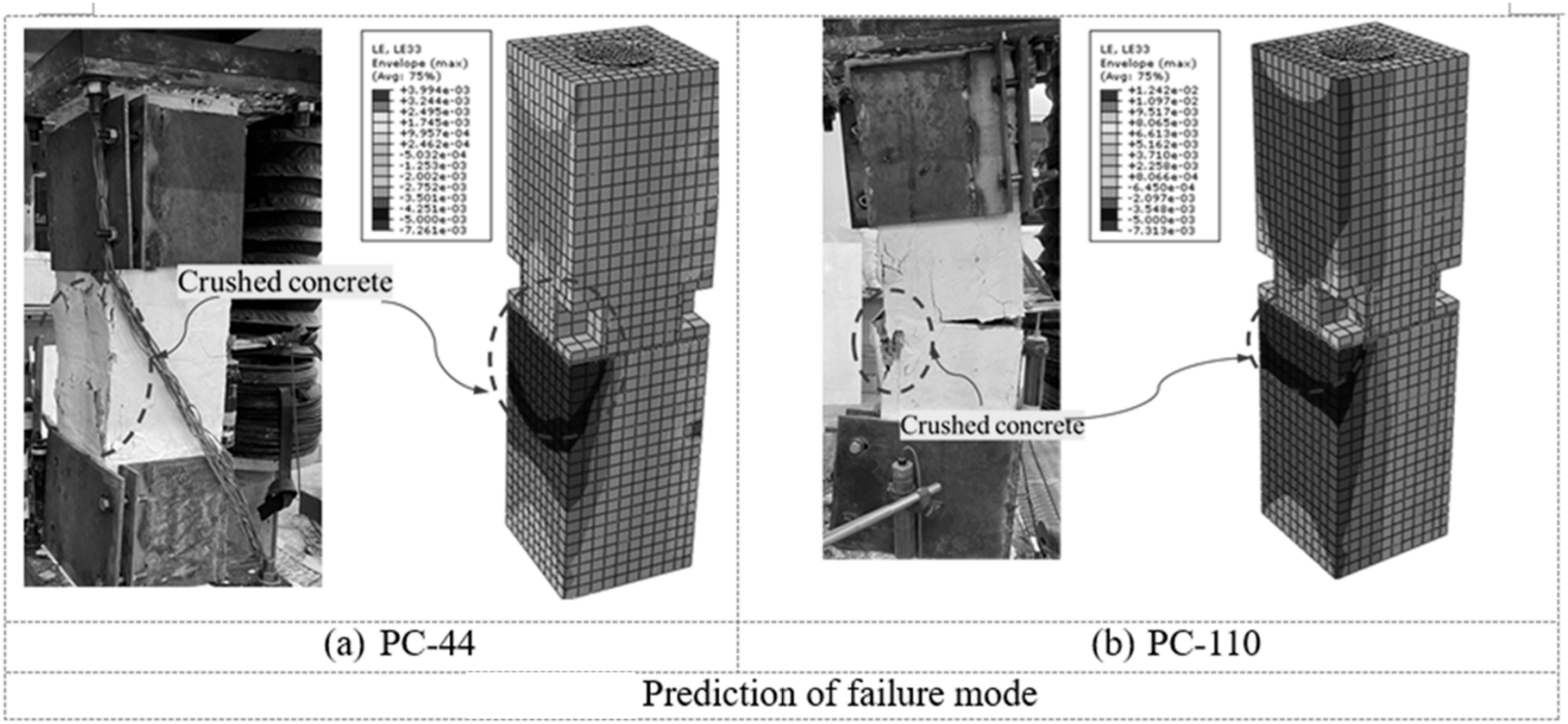
LE, LE33
Envelope (max)
(Avg: 75%)
+3.994e-03
+3.244e-03
+2.495e-03
+1.745e-03
+9.957e-04
+2.462e-04
-5.032e-04
-1.253e-03
-2.002e-03
-2.752e-03
-3.501e-03
-4.251e-03
-5.000e-03
-7.261e-03
Crushed concrete
LE, LE33
Envelope (max)
(Avg: 75%)
+1.242e-02
+1.097e-02
+9.517e-03
+8.065e-03
+6.613e-03
+5.162e-03
+3.710e-03
+2.258e-03
+8.064e-04
-6.450e-04
-2.097e-03
-3.548e-03
-5.000e-03
-7.313e-03
Crushed concrete
(a) PC-44
(b) PC-110
Prediction of failure mode

Fig. 45

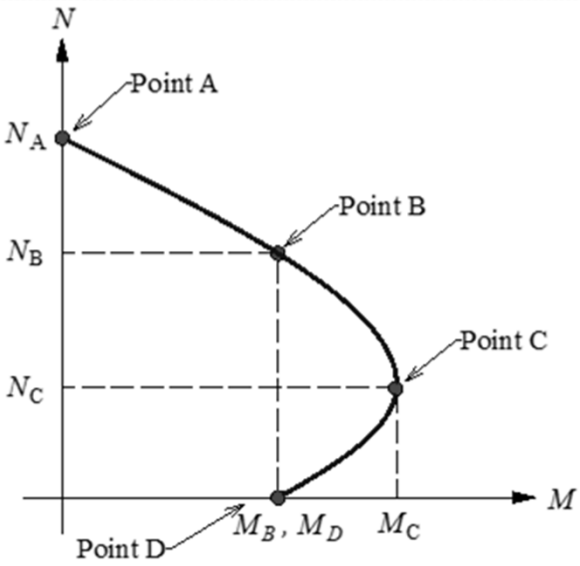

Typical *N-M* interration curve of columns

Fig. 46

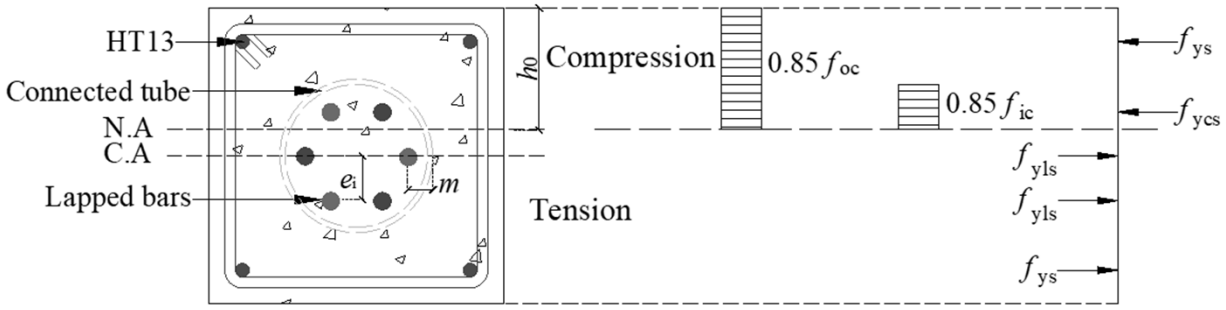

Plastic stress distribution of cross-section-Connection interface

Fig. 47

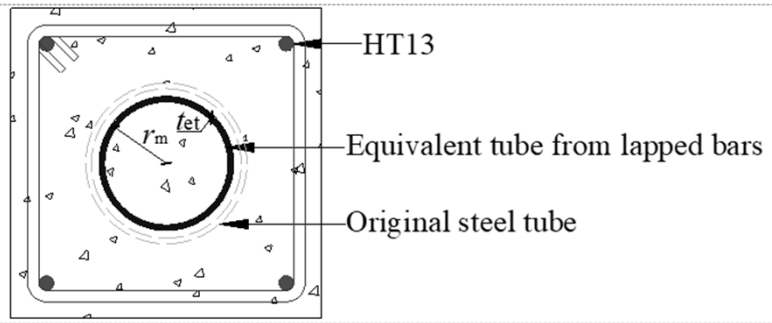

Transformed cross-section of precast connection

Fig. 48

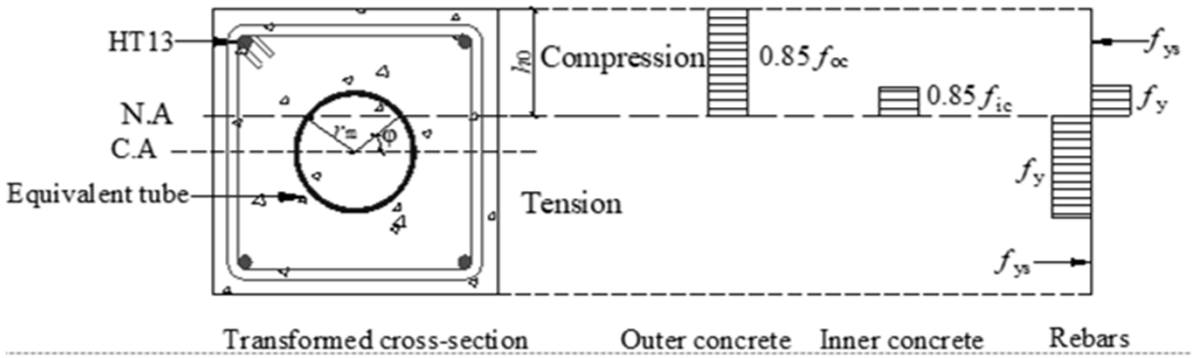

Neutral axis within steel tube

Fig. 49

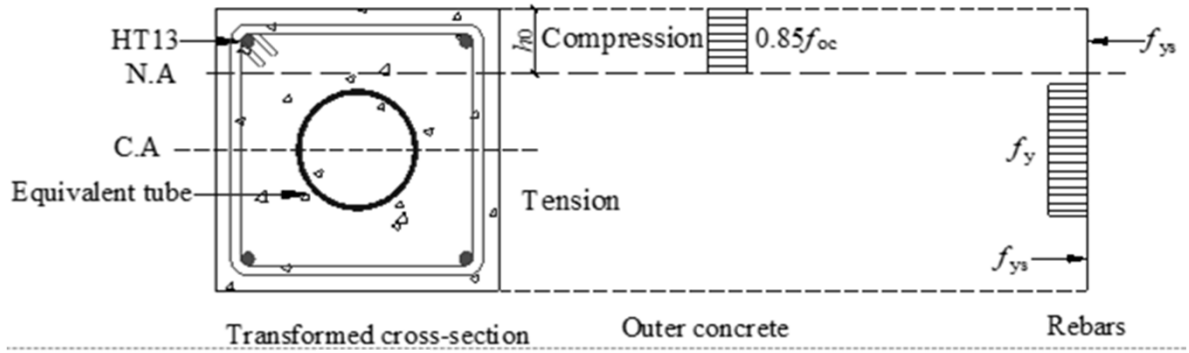

Neutral axis outside steel tube

Fig. 50

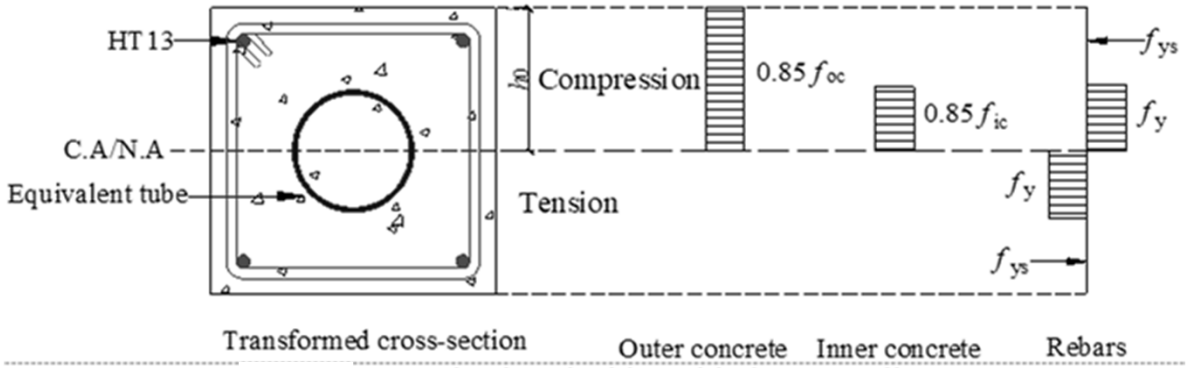

Neutral axis coincides with the centre line

Fig. 51

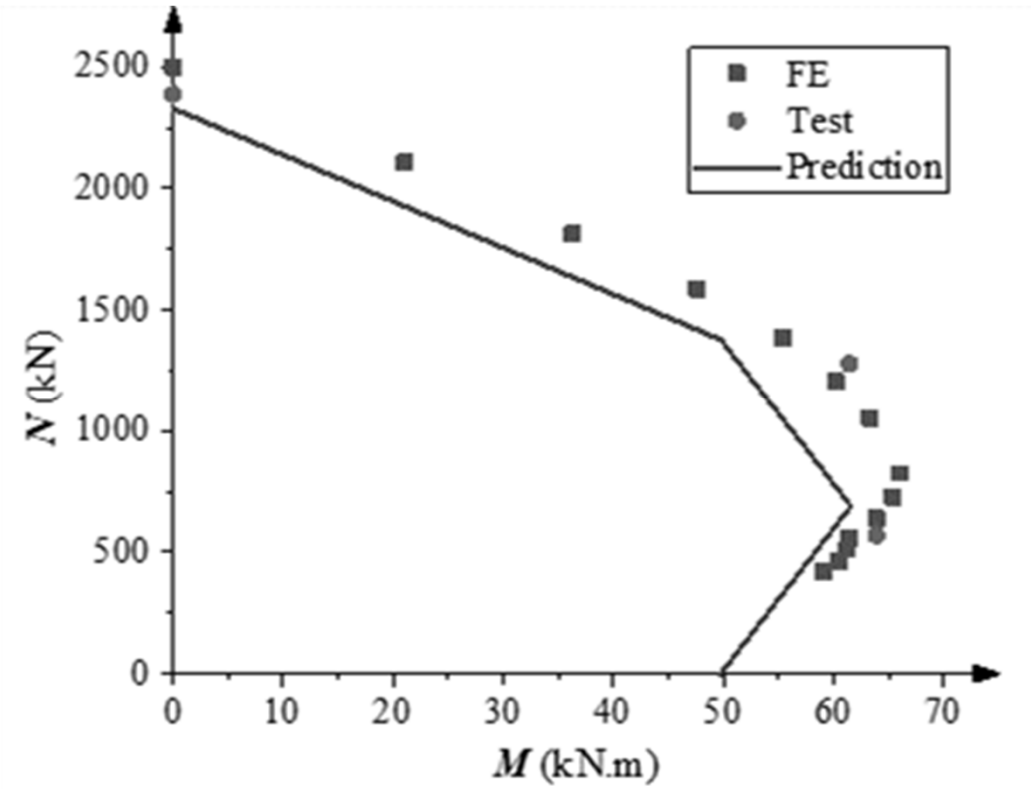

Comparison between model predictions
and experimental and numerical results

Fig. 52